**The Thesis Committee for Erwan Chabert**
**Certifies that this is the approved version of the following thesis:**

# SIMULATION AND ANALYSIS OF THE MULTIPHASE FLOW AND STABILITY OF CO-EXTRDUED LAYERED POLYMERIC FILMS

**APPROVED BY**
**SUPERVISING COMMITTEE:**

**Supervisor:**

Roger T. Bonnecaze, Supervisor

Don R. Paul

# Simulation and analysis of the multiphase flow and stability of co-extruded layered polymeric films

**by**

**Erwan Chabert, BSE**

**Thesis**

Presented to the Faculty of the Graduate School of

The University of Texas at Austin

in Partial Fulfillment

of the Requirements

for the Degree of

**Master of Science in Engineering**

**The University of Texas at Austin**

**August 2011**

# Dedication

To my family,

Je ne vous dis pas assez que je vous aime.

To my supporting friends,

# Acknowledgements

My first and biggest acknowledgement must go to my advisor, Dr. Roger T. Bonnecaze. He is an outstanding mentor and a remarkable advisor. He has always been supportive, patient and available despite his very busy schedule as department chair. He managed to keep me motivated and positive about my research at every step along the way. He really cares about his students' well being both inside and outside of the office. I was really fortunate to learn from him and I would be very happy if he has found our relationship a tenth as fulfilling for him as I think it has been for me. I am also grateful to him for accepting my challenges on the squash court. I always lost but I will not stop trying.

Acknowledgments go to the wonderful research group I have been a part of. Special thanks must go to Lavanya Mohan and Derek Basset with whom I have shared an office and laughter during these two years. They were always very helpful and willing to answer my questions.

I would like to thank Dr. Donald R. Paul for reading this thesis. I'm also thankful for his "introduction to polymer science" course which helped me a lot towards my research.

I would also like to thank Randy Rife who was always available to help me solve the problems with my computer, even at the very last moments before turning this thesis.

Finally, I would like to thank my French peers (Claire, Gwennael, Mathieu, Philippe and Maria) and all the wonderful people I have met here who helped me keep my sanity, especially my theater friends from Winedale, Foot in the Door and Madrigal Dinner.

# Abstract

## Simulation and analysis of the multiphase flow and stability of co-extruded layered polymeric films

Erwan Chabert, MSE

The University of Texas at Austin, 2011

Supervisor: Roger T. Bonnecaze

The flow and stability of co-extruded layers of different polymers in a forced assembly process is studied computationally to determine the extent of the stable process window and the types of instabilities that occur. Recent advances in layer-multiplying co-extrusion of incompatible polymers have made possible the fabrication of multilayered nanostructures with improved barrier, thermal and mechanical behavior. However, existing layering techniques are very sensitive to mismatches in viscosity and elasticity of the co-extruded polymers which often give rise to layer non-uniformity and flow instabilities, such as encapsulation. Simulations of the flows inside the feedblock and the successive multiplier dies of the multi-layering system are used to track the interface and predict instabilities and degrees of encapsulation as a function of process parameters, primarily the flow rates and rheology of the polymers. Encapsulation is found to be negligible in practice in the feedblock even for large viscosity contrasts and differences in elasticity between the two co-extruded polymers. Encapsulation or pinch-off of interfaces is more severe in the multiplier dies when there the rheologies of the polymers differ. A secondary flow due to the second normal stress differences for non-

Newtonian fluids is primarily responsible for the encapsulation. A new multiplier design is proposed and simulated. The pressure drop in the proposed design is half that of the current design, which is useful for extruding highly elastic materials. Further, the degree of encapsulation is also reduced. The results of the simulations are validated with experimental measurements of pressure drop and flow visualization provided by research collaborators.

# Table of Contents

# List of Tables

# List of Figures

# Chapter 1: Introduction

Materials are often combined to make a composite material with superior properties, ideally the best of the starting components. Combining polymers and other components has created new materials with interesting and valuable properties and opened new possibilities for engineering applications. Examples include polymer composites by addition of particles or fibers to polymer (Bucknall 1997; Li *et al.* 2010), polymer blends (Utracki 2002, Strobl 2007) made by mixing one or more polymers, and block copolymers which are two or more different polymer chains chemically linked (Balta Calleja & Roslaniec 2000).

One method to produce composite materials is through multilayering components by coextrusion processes, where two or more polymers are extruded and joined together. This technique can be generalized to manufacture materials with several thousand layers, with thicknesses ranging from microns to nanometers.

## 1.1 Current and potential applications

Multilayered polymers are used in a variety of applications, including coloring (Xie *et al.* 1999; Bluem *et al.* 2009), UV protection (Kynar Films 2001) and as less expensive and superior alternatives to materials like metals, textiles, glass or paper (Dooley 2002). Current markets for multilayered coextruded products include food packaging, membranes for gas separation and water purification. Multilayered polymers can offer better selectivity for gas separation. Nanolayers of EAA (poly(ethylene-co-acrylic acid)) with small domains of PEO (poly(ethylene oxide)) in the rubbery state produces superior gas barrier materials (Pethe *et al.*, 2008). The impact on oxygen

scavenging of a multilayered structure as opposed to a homogeneous one or a polymer blending has also been extensively studied (Carranza 2010).

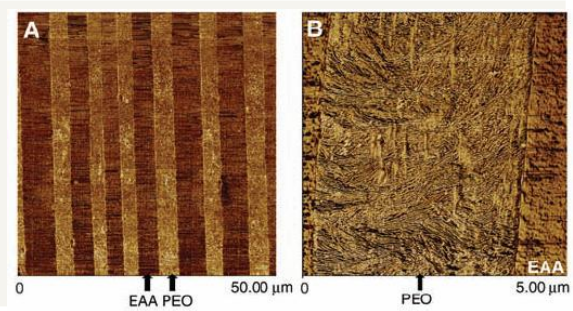


**Figure 1.1** PEO (crystallized)-EAA multilayered structure for enhanced gas barrier. Image from Wang *et al.* (2009).

Multilayering techniques allow the creation of materials with superior mechanical and optical properties (Ponting *et al.* 2010a). These new applications include, for example, 3-D optical data storage to attain the terabit storage capability on a DVD-size disk and advanced optical filters and organic lasers that can find applications in sensing, display and lighting. For example, multilayered resonators consisting of 128 alternating layers of PMMA and PS were used as resonators (Singer et al. 2008) in organic lasers (Samuel 2004) that are easier to fabric and shape than inorganic lasers. The lasing wavelength can be controlled via the layer thickness.

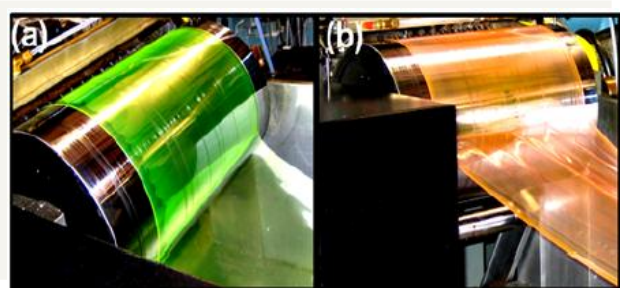


**Figure 1.2** Nanolayered lasing material. Image from Song *et al.* (2009).

Being able to vary the composition of a nanolayered polymer film with layer thickness less than a fourth of the wavelength enables the creation of films of controlled refractive indexes while keeping them transparent (Ponting *et al.* 2010a).

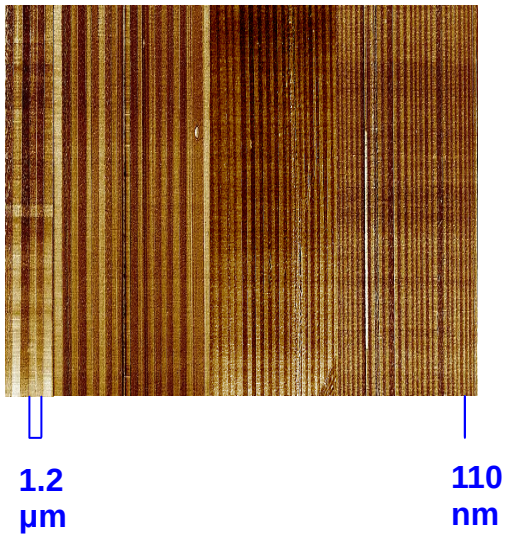


**Figure 1.3.** Variable refractive index filmsfor GRIN lenses and optical filters. Image from Ponting *et al.* (2010a).

Finally, a multilayered structured material can have improved mechanical properties. Multilayered PVA/silica composites have been synthesized, and an increase in the tensile strength and ductility has been observed (Li *et al.* 2010).

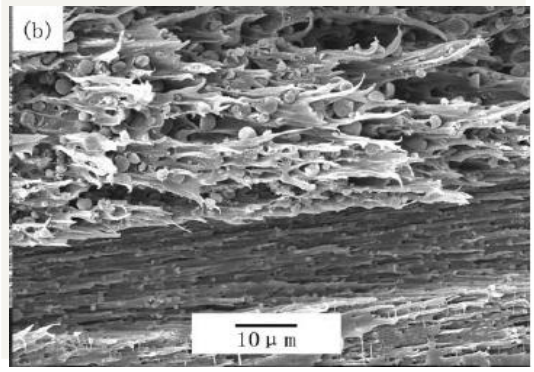


**Figure 1.4**. Surface morphology of monolayered PVA/silica composite of improved ductility and strength from Li *et al.* (2010).

## 1.2 MULTILAYERING TECHNIQUES

Multilayer coextrusion processes are very attractive technically and economically as they are a one-step process compared to lamination and coating processes. The latter require complex and expensive steps to make each individual ply, prime, coat and laminate them (Dooley 2002).

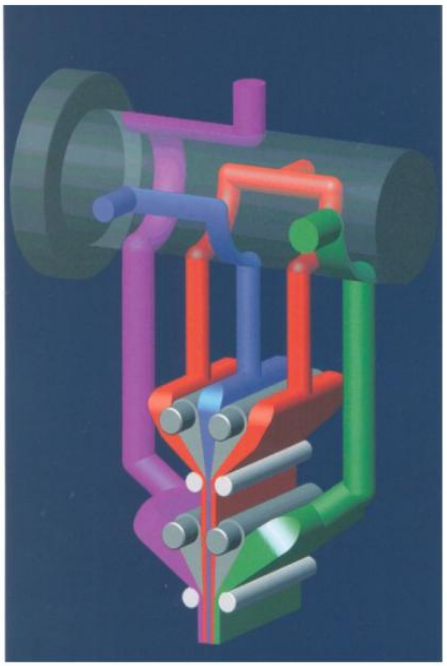

**Figure 1.5**. Illustration of a lamination and coating process (from Cloeren technology).

In every multilayer coextrusion process, two or more polymers are extruded, shaped and joined together in a die so that a multilayer film can be formed. Many different methods are currently in practice to manufacture multilayered systems. There are several methods for producing multilayered polymer films (Raley 1965; Chisholm & Schrenk 1971; Wooddell 1980; Schrenk 1992; Dooley 2002). The two most common methods use tubular blown films dies and flat dies (Dooley 2002).

The tubular-blown film processes was one of the earliest methods used to make multilayered polymer composites (Raley 1965). The polymers are extruded in concentric

rings and join together while air is blown in the center to cool down and solidify the polymer film. Controlling layer thicknesses, especially for increasing number of layers, require a skilled technician.

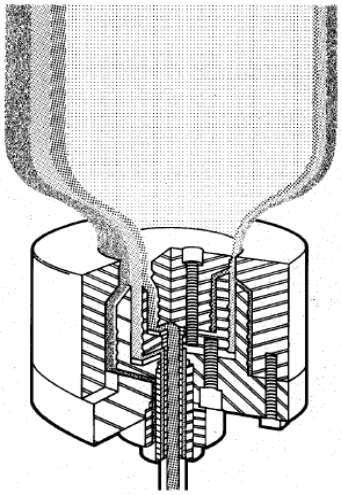

**Figure 1.6**. Illustration of a three-layer blown film die/ tubular coextrusion from Dooley (2002).

Another process is the feedblock method of flat-die coextrusion patented by the Dow Chemical Company (Chisholm & Schrenk 1971). It combines a feedblock with as many inputs as the desired number of layers and a die that reduces the thickness of the layers while spreading it and extending its width.

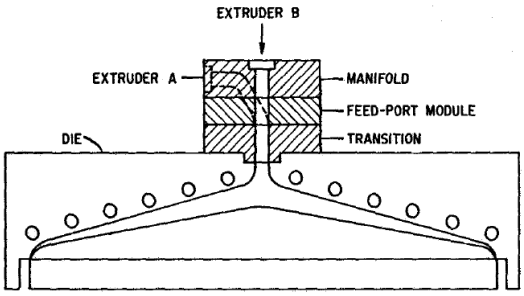


**Figure 1.7**. A feedblock and die combination from Dooley (2002).

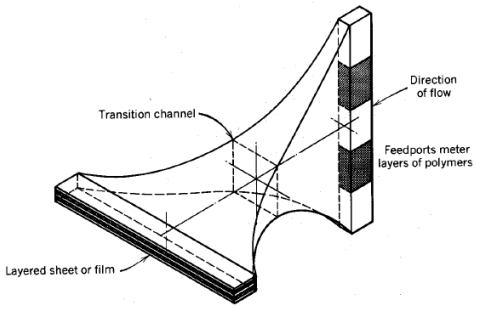


**Figure 1.8**. A 4-layers coextrusion process from Dooley (2002).

This thesis focuses on another type of multilayering method, developed at Case Western Reserve University (Ponting *et al.* 2010a) and now in the Center for Layered Polymer Systems (CLiPS) (Ponting *et al.* 2010b). It is based on a process of forced assembly using a series of layer multiplication dies to fabricate thin (from the micron to the nanometer scale) alternating layers of two or three polymers. What makes this coextrusion process unique is the combination of a conventional coextrusion in a feedblock and the successive layer multiplications by multiplier dies.

Like methods discussed previously, the process presented in this thesis is currently well controlled only for materials with low elasticity and of similar viscosities. The goal is to apply the multilayering technique to a broader range of materials. More viscous and more elastic fluids are more difficult to process since, as an example, larger pressure drops are necessary to extrude these fluids.

## 1.3 CLIPS METHOD

### 1.3.1 Process

The CLiPS multilayering system consists of extruders, pumps, a feedblock, multiplying dies, surface layer extruders and an exit die as is illustrated in Figure 1.9 for a three component polymer system.

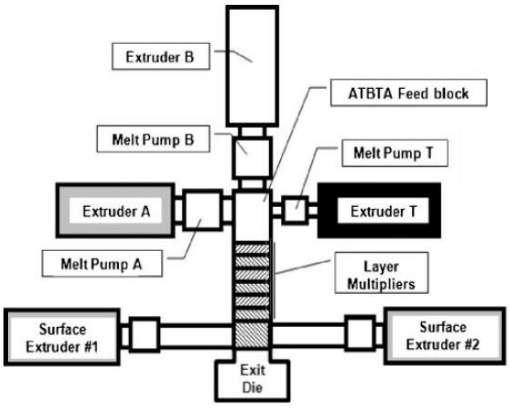


**Figure 1.9.** Overall schematic of the multilayering process presented in this thesis from Ponting *et al.* (2010a).

The three polymer layers are extruded and joined together in a feedblock. It is followed by one to several multiplier dies in a row that multiply the layers as many times as desired by successive stacking.

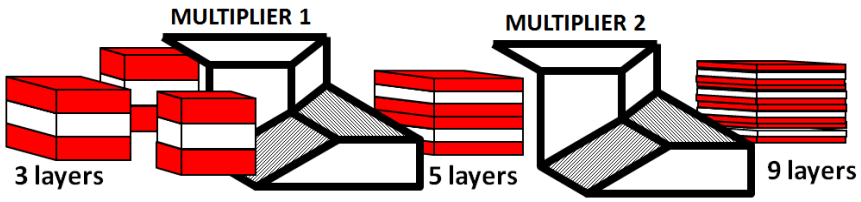


**Figure 1.10**. Schematic illustration of 2 mulitpliers for a two-component material.

Figure 1.10 illustrates how a two-component coextrusion through one multiplier element increases the number of layers from 3 to 5. Another multiplier die increases again the number of layers. Figure 1.11 shows the working principle of the die for a two-component extrusion. The element at the input is cut, spread and recombined to double the number of layers.

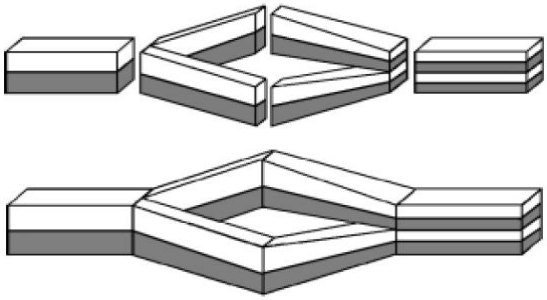

**Figure 1.11**. Illustration of the function of a multiplier from Dooley (2002).

This ability of putting in series as many multiplier elements as desired gives total control on the obtained number of layers of the manufactured product as Table 1.1 and Figure 1.12 summarize.

| Number of layers for | AB system | | ABC system | | ABA system | |
|---|---|---|---|---|---|---|
| Only Feedblock | 2 | 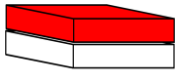 | 3 | 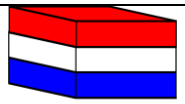 | 3 | 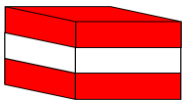 |
| Feedblock + 1 multiplier | 4 | 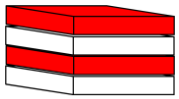 | 6 | 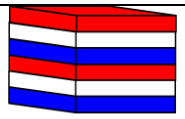 | 5 | 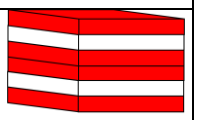 |
| Feedblock + N multipliers | $2^{N+1}$ | | $2^{N+2}+1$ | | $2^{N+1}+1$ | |

**Table 1.1**. Number of layers at the exit according to the number of multipliers with two different polymers at the inputs of the feedblock.

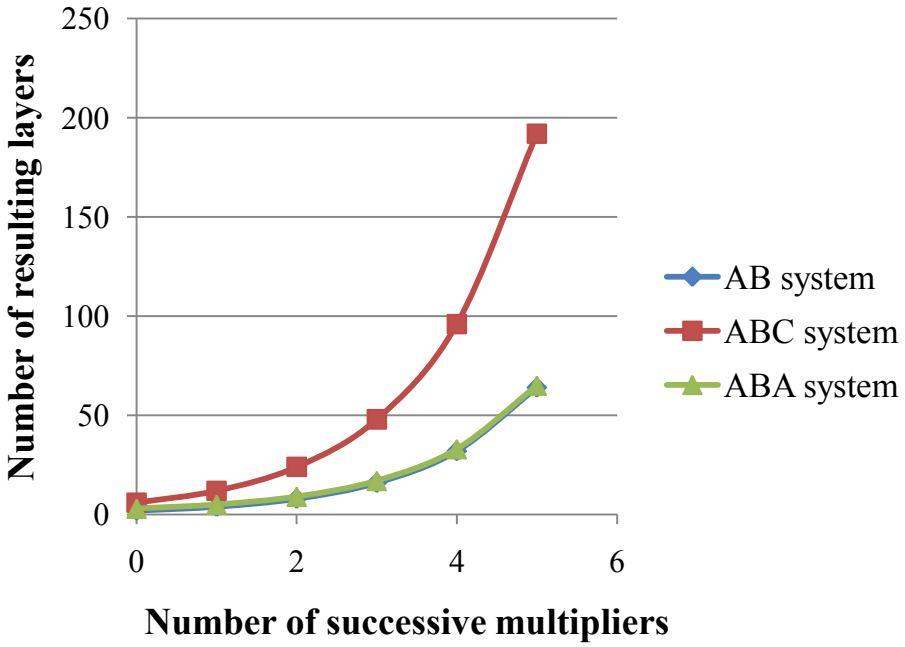


**Figure 1.12**. Number of layers versus number of multipliers.

### 1.3.2 Instabilities

Thickness uniformity and flatness of the layers are essential to manufacture a product with uniform properties. Polymer rheology is more complex than Newtonian rheology because of the shear rate dependence and elasticity. This complex behavior adds

other potential instabilities (elastic instability, elastic recoil) to those that already occur for Newtonian fluids (encapsulation, waves) during the coextrusion process. Interfacial distortions consist in a local variation of the interface location and can occur for different reasons. It can be due to flow instability, a mismatch in viscosity or due to the viscoelastic nature of the fluid (Southern & Ballman 1973; White & Lee 1975; Everage 1975; Su & Khomami 1992A, 1992B; Wilson & Khomami 1993; Khomami & Wilson 1995; Ramanathan *et al.* 1996; Dooley 2002; Yue *et al.* 2008). Figure 1.13 illustrates the different types of instabilities that can be distinguished.

a. from Dooley (2002)

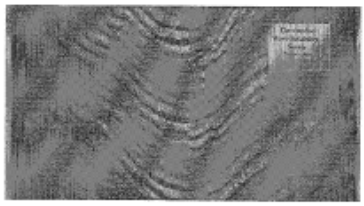

b. from Dooley (2002)

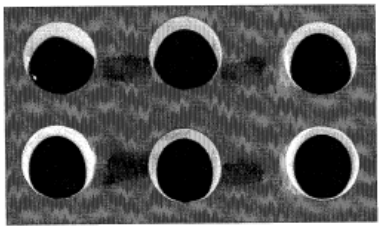

c. from Dooley (2002)

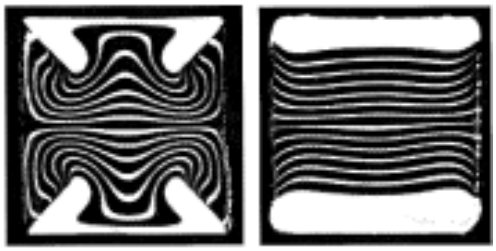

d. from Ponting *et al.*(2010)

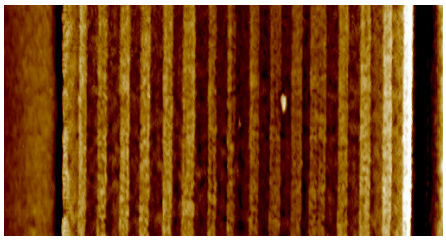

**Figure 1.13**. Potential multilayering instabilities. a) distortion of the interface between the different polymers; b) encapsulation of the more viscous fluid (black) by the less viscous fluid (white); c) elastic instability occurring in 2 component multilayering extrusion: second normal stress differences create secondary flow that can "mix" the polymer layers in non-radially symmetric channels; d) multilayering of 2 different polymers in which elastic recoil occurs, causing variations in layer thickness (here 15%)

### *1.3.2.1 Interfacial distortion*

At a certain flow rate, waves on the interface can be observed (Ramanathan *et al.* 1996; Everage 1975). They can dramatically grow with a higher flow rate that can yield to the formation of a fold (zig-zag instability). Interfacial tension between the two polymers can also create waves on the interface (Figure 1.13a).

### *1.3.2.2 Encapsulation*

Mismatch of viscosities can cause encapsulation instabilities (Figure 1.13b). The fluid of lower viscosity migrates to regions of highest shear, *i.e.* to the wall of the die as it moves downstream from left to right and from top to bottom (Southern & Ballman 1973; Dooley 2002; Yue *et al.* 2008). It therefore tends to encapsulate the fluid of higher viscosity. It can make a core/outer layer type of flow and happens in both cylindrical and rectangular dies. That is why multilayer coextrusion currently requires similar polymer viscosities for uniform layering. This is achieved either by using polymers of similar viscosity at the same temperature or by raising the temperature of one polymer to match the other's viscosity.

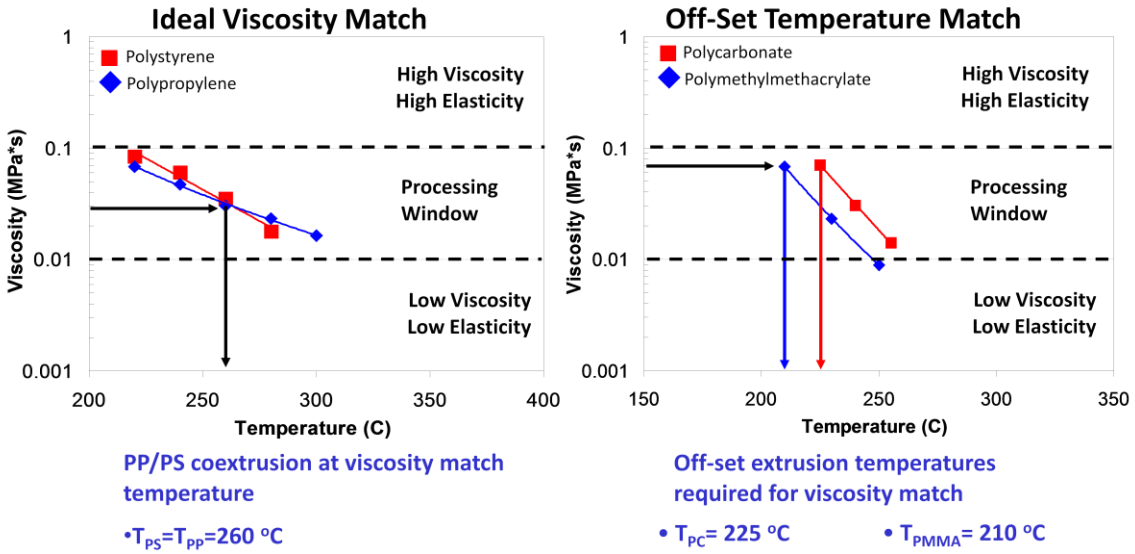


**Figure 1.14**. Viscosity matching (similar polymer or thermally controlled viscosity).

#### *1.3.2.3 Elastic instability*

Even when viscosities of polymer match, layer deformation can occur. Studies showed that second normal stress differences create secondary flows normal to the primary flow direction (Debbaut *et al.* 1997; Dooley 2002; Wilson & Khomami 1993). The latter can distort the layer interface and "mix" the polymer layers in non-radially symmetric channels causing a layer rearrangement (Figure 1.13c).

#### *1.3.2.4 Elastic Recoil of the Extrudate*

Elastic stresses at the processing boundaries affect layer uniformity and surface topology (Figure 1.13d).

## 1.4 THESIS GOALS

This research is part of the Center for Layered Polymeric Systems (CLiPS) and aims to improve the current coextrusion technique. In fact this process is currently effective only for few pairs of polymers for which the instabilities presented in 1.3.2 are somewhat controlled by, in particular, matching the fluids' viscosities. However, in order to expand the process window so that new applications (cf. 1.1 ) can be enabled, a better understanding of the fluid flows with respect to the fluid parameters as well as with the design of the dies is required. Expanding the process window and coextruding layered polymers with layer thicknesses down to the nanoscale would create even more opportunities to discover unique properties.

To be able to generalize this process to more polymers, we have developed computational simulations of flows in the feedblock and the multiplier dies and studied the flows of different pairs of fluids through simulations. Different designs of channels are evaluated to help in the stabilizing control (flatness, thickness regularity) of the

layers. The results of these simulations will give information on how the channel designs affects the interfaces and will guide the design of new dies and suggest modifications of processing to give a satisfactory product.

## 1.5 THESIS OUTLINE

The outline for the remainder of the thesis is as follows. In chapter 2 the simulated system and simulation methods are described. The geometries of the feedblock and the multiplier dies are presented. The constitutive equations governing the fluid flow are described and the model characterizing the non-Newtonian behavior of the polymers is introduced.

Chapter 3 presents the simulations of flow in the feedblock for both (described using the Phan-Tien-Tanner viscoelastic model). The position of the interfaces between the polymers, instabilities and degrees of encapsulation are determined as a function of process parameters.

In chapter 4 the flow of Newtonian and non-Newtonian fluids are simulated for multiplier dies. Two different geometries are studied to compare the effects of changes in geometry on pressure drop and layer stability.

Chapter 5 presents conclusions and recommendations for future work.

# Chapter 2: Model for forced polymer layering process

## 2.1 INTRODUCTION

This chapter details the function, the geometry and the dimensions of the feeblock and multiplier dies. This chapter also presents the fluid mechanical model and parameters used for the simulations discussed in chapters 3 and 4. An ABA extrusion is the extrusion of a three layered material with material A on top and bottom the and material B in the middle. An ATBTA material is the successive layers of materials A T, B, and T and A.

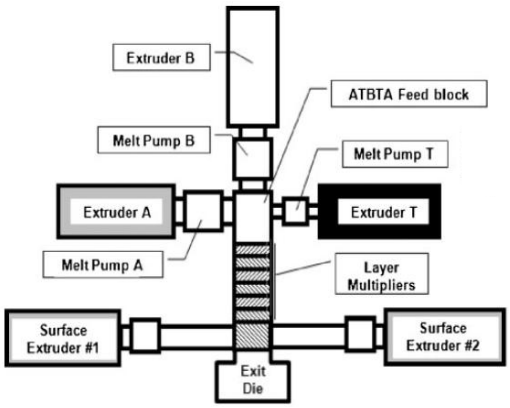


**Figure 2.1.** Overall schematic of the multilayering process presented in this thesis from Ponting *et al.* (2010a).

As explained in chapter 1, the multilayering process consists of the extrusion of the polymers through the feedblock where they are layered and followed by multiplier dies that increases the number of layers by cutting and stacking them one on top of the other (Figure 2.1). Other multipliers can be added successively to increase the number of layers. Figure 2.2 illustrates the idealized geometry of the multilayering system.

The simulations in this thesis focus on the feedblock and the first multiplier.

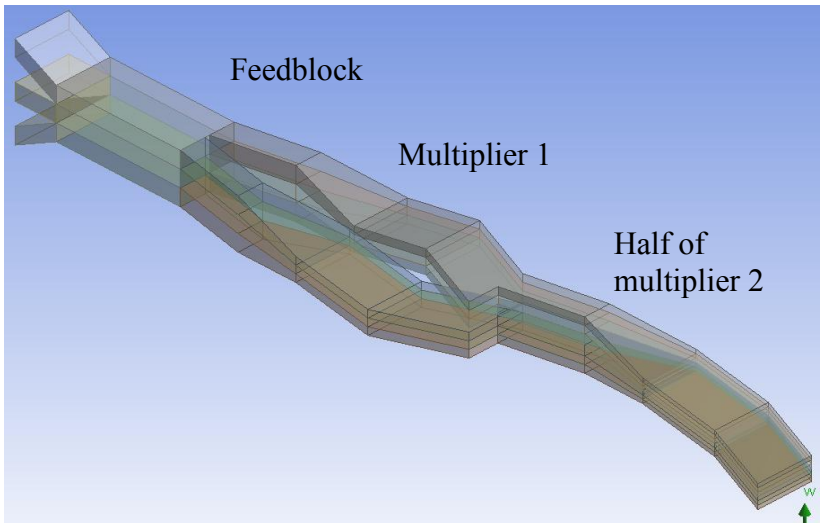


**Figure 2.2.** Geometry of the feedblock and two successive (new) multipliers modeled in DesignModeler (Ansys). Only half of the second multiplier is shown for clarity.

## 2.2 FEEDBLOCK

Extruders melt the polymers with typical processing temperatures of 200 to 300$^{o}$C and inject the melt into the feedblock (Figure 2.2). The feedblock can coextrued up to five different polymers as shown in the design of the feedblock in Figure 2.3. The focus of the simulations of the feedblock in this thesis is on the channel (framed in red) from its inlet to the input of the first multiplier.

This study is limited to the three inputs, particularly the cases of producing ABA layered structures. For an ABA multilayered structure, only two extruders are necessary because the network of channels can feed both the top and bottom layers.

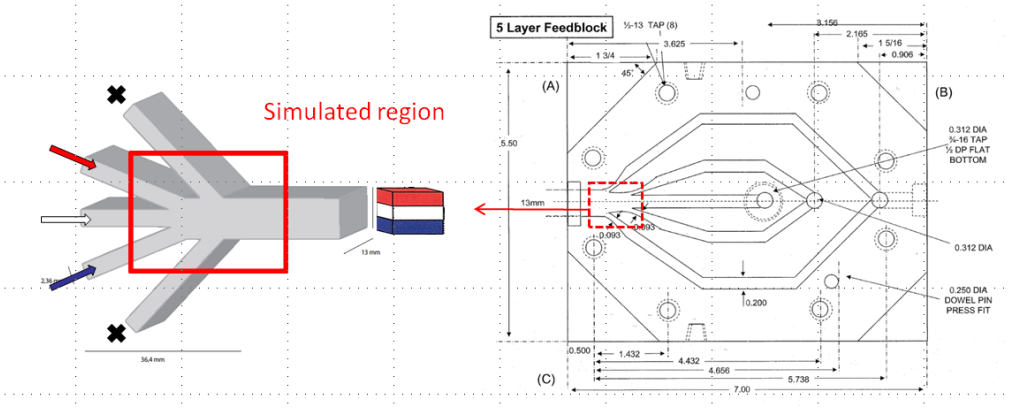


**Figure 2.3.** Blue print of the 5 layers feedblock and focus of the simulation.

Figure 2.4 presents the dimensions of the feedblock on which the idealized geometry for the simulation has been inspired. It shows two planes of symmetry. Experimentally, the outside layers have the same flow rate (8 rpm = 1.6 x 10-7 $m^3$ $s^{-1}$) and the inner layer flow rate is slower (6 rpm =1.2 x 10-7 $m^3$ $s^{-1}$) so that the velocity of the polymer melt is the same throughout all the melt. All the inputs have the same width but naturally layer thicknesses are dependent on the flow rates of each input.

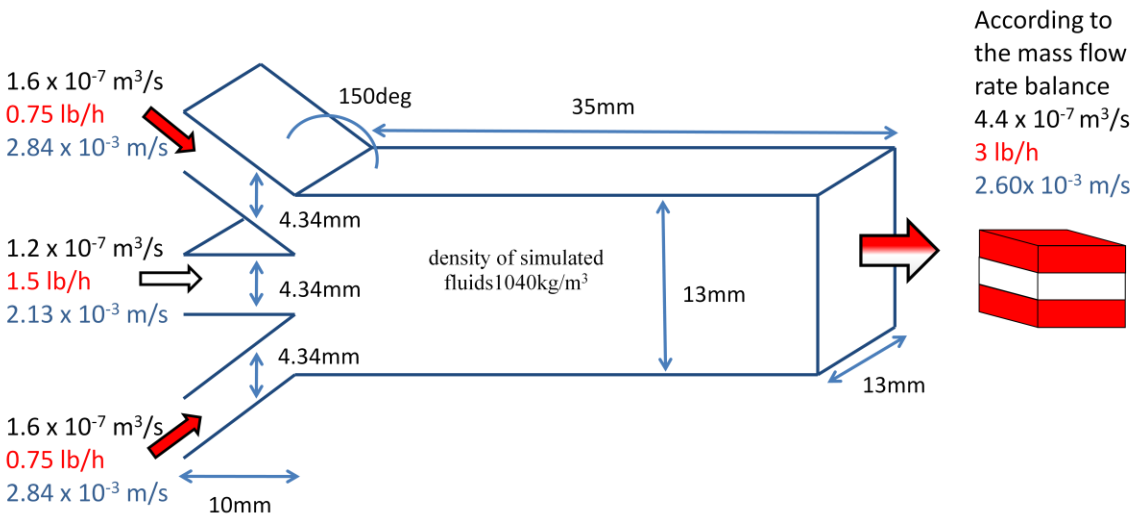


**Figure 2.4.** Feedblock sketch with dimensions and parameters

The desired output at the exit of the feedblock is multilayered product with uniform thicknesses. Chapter 3 presents the simulations of the flow inside the feedblock. Simulations will provide an understanding of the potential instabilities, pressure drop and general fluid dynamics in the feedblock that determine the processing window.

## 2.3 MUTLIPLIER DIE

### 2.3.1 Function

The multiplier constitutes the second part of the multilayering process. After the feedblock coextrudes the polymers several multipliers cut and restack the polymers to make the multilayered material. The more multipliers the more layers are produced.

This process is illustrated in Figure 2.5. The layered polymer is first split laterally into two parts (step A). Each part is then channeled one on top of the other through two independent dies (step B). The channel widens to recover the same width as at the input (step C). Finally, the two parts, now split horizontally are merged to "multiply" the layers (step D).

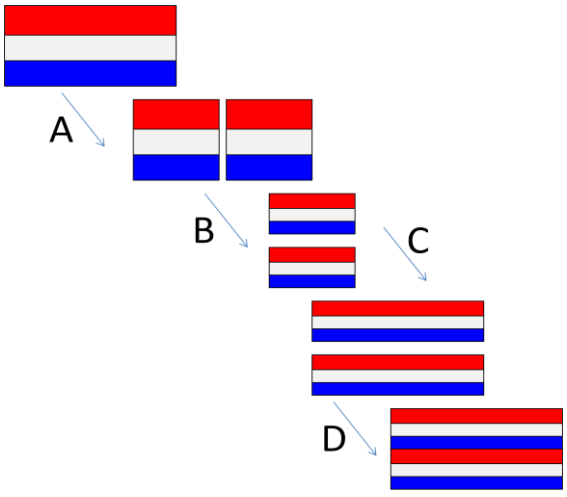


**Figure 2.5.** ABA Schematic of the layer multiplication process.

### 2.3.2 Geometry and parameters

Two different multiplier die geometries have been studied (Figure 2.6 and Figure 2.7). The curved geometry in Figure 2.6 is referred to as the "current" geometry as it is currently used at Case Western Reserve University as of the submission of this thesis. The other design in Figure 2.7 is the other one is referred as "new" as it is a new proposed design.

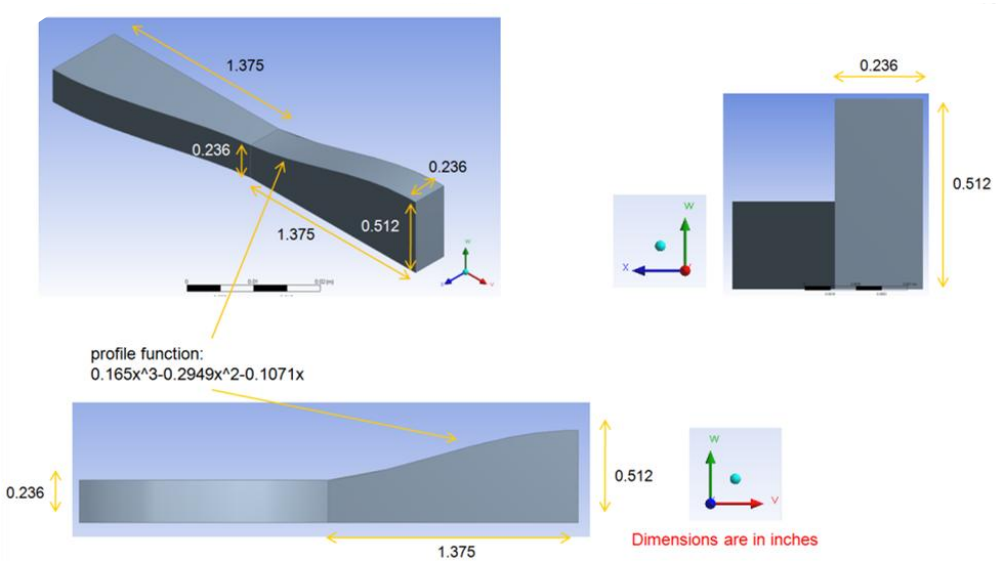


**Figure 2.6.** Current multiplier die geometry.

For the simulations in this thesis three layers enter the first multiplier die from the feedblock. However, since the outflow of the feedblock is split in two, the flow rates are twice as small as in the multiplier. Top and bottom layer then enter with a flow rate of 8.0 x $10^{-8}$ $m^3/s$ and the middle layer has a flow rate of 6.0 x $10^{-8}$ $m^3/s$.

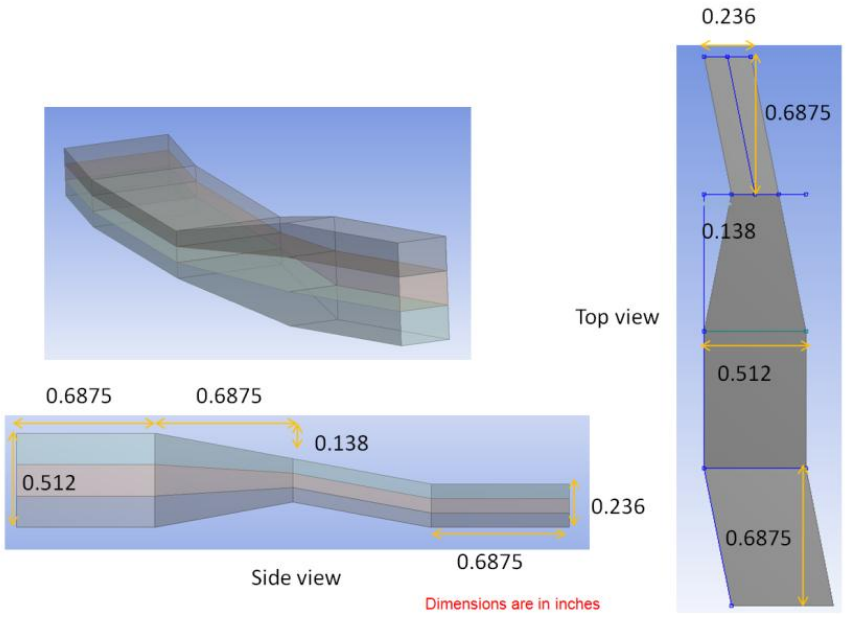


**Figure 2.7.** New multiplier die geometry.

Chapter 4 presents the simulations that have been conducted to better predict and understand the fluid flows in the multiplier.

## 2.4 MODEL FOR SIMULATIONS

### 2.4.1 Choice of the model

Several models have been proposed to describe the constitutive behaviors of polymer melts (*e.g.,* Phan-Thien-Tanner, Giesekus, and Oldroyd-B models). We use the Phan-Thien-Tanner (PTT) model because of its very good fit to experimental rheological data on typically extruded materials (Phan-Thien & Tanner 1977). Measurements with shear and extensional rheometers have been conducted and a good agreement between experiments and the PTT model has been found as shown in Figure 2.8.

a.

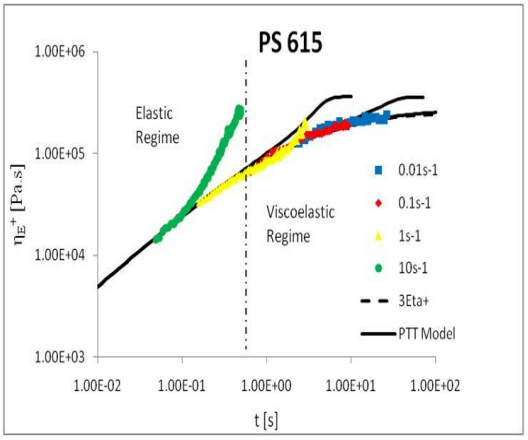


b.

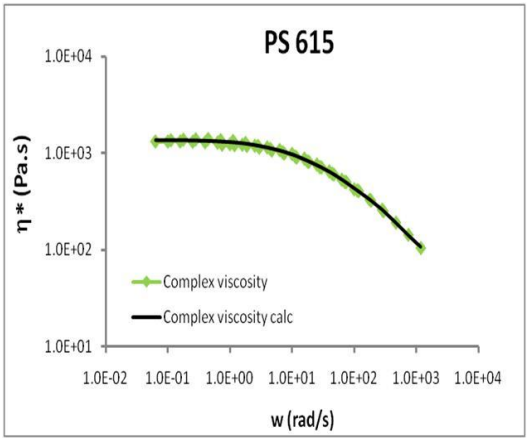


c.

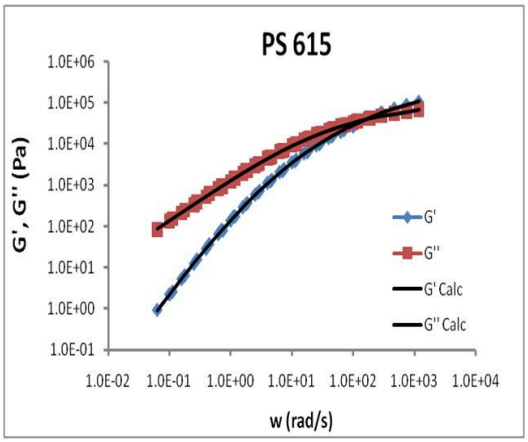


**Figure 2.8.** Viscoealstic characterization of polystyrene PS615 from the Dow Chemical Company. a) extensional characterization at 160C; b) and c) shear characterization at 220C. The Maia group at Case Western Reserve University determined that the experimental behavior of the polymer can be well characterized with 4 modes.

### 2.4.2 Equations of motion, constitutive equations and parameters

#### *2.4.2.1 Equations of motion*

The equations governing incompressible isothermal flows are the Cauchy-momentum equation in three dimensions given by

$$\rho \frac{D\mathbf{u}}{dt} = \nabla \cdot \mathbf{T} + \nabla p + \rho \mathbf{g} \tag{2.1}$$

and the continuity equation

$$\nabla \cdot \mathbf{u} = 0, \tag{2.2}$$

where $t$ is the time, $\mathbf{u}$ is the velocity vector, $p$ is the pressure, $\rho$ is the fluid density, $\mathbf{g}$ is the gravitational field and $\mathbf{T}$ is the stress tensor described by the PTT model.

#### *2.4.2.2 Phan-Thien-Tanner (PTT) constitutive equation*

The tensor $\mathbf{T}$ is split into a viscoelastic component $\mathbf{T}_1$ that is computed according to the chosen PTT model (Phan-Thien & Tanner 1977) and a purely viscous term $\mathbf{T}_2$. (This decomposition helps the convergence of the numerical method (Ansys POLYFLOW user's guide)). Therefore, the stress $\mathbf{T}$ is given by

$$\mathbf{T} = \mathbf{T}_1 + \mathbf{T}_2 . \tag{2.3}$$

$\mathbf{T_2}$ is considered as the stress response associated with the fastest relaxation time and $\eta_2$ is the viscosity factor associated with it so that

$$\mathbf{T}_2 = 2\,\eta_2\,\mathbf{D}. \tag{2.4}$$

$\mathbf{T_1}$ according to the PTT model is implicitly given by

$$\exp\left(\frac{\varepsilon\lambda}{\eta_1}\mathbf{T}_1\right)\mathbf{T}_1 + \lambda\left[\left(1-\frac{\xi}{2}\right)\overset{\nabla}{\mathbf{T}}_1 + \frac{\xi}{2}\overset{\Delta}{\mathbf{T}}_1\right] = 2\,\eta_1\,\mathbf{D}. \tag{2.5}$$

The symbol $\overset{\nabla}{\mathbf{T}}_1$ the upper-convected time derivative of $\mathbf{T}_1$, and $\overset{\Delta}{\mathbf{T}}_1$ is the lower-convected time derivative of $\mathbf{T}$ where

$$\overset{\nabla}{\mathbf{T}} = \dot{\mathbf{T}} - \nabla\mathbf{v}^T \cdot \mathbf{T} - \mathbf{T} \cdot \nabla\mathbf{v}, \tag{2.6}$$

and

$$\overset{\Delta}{\mathbf{T}} = \dot{\mathbf{T}} + \nabla\mathbf{v}^T \cdot \mathbf{T} + \mathbf{T} \cdot \nabla\mathbf{v}. \tag{2.7}$$

The rate of deformation tensor $\mathbf{D}$ is expressed as

$$\mathbf{D} = \frac{1}{2}(\nabla\mathbf{v} + \nabla\mathbf{v}^T). \tag{2.8}$$

The viscosity $\eta_1$, is given by

$$\eta_1 = (1 - \eta_r)\eta \ , \tag{2.9}$$

$$\eta = \eta_2 + \eta_1, \tag{2.10}$$

With the viscosity ratio $\eta_r$ given by

$$\eta_r = \frac{\eta_2}{\eta_2 + \eta_1}. \tag{2.11}$$

Finally $\lambda$ is the relaxation time; $\varepsilon$ is an extensional parameter while $\xi$ affects the shear behavior.

The equation (2.5) is written in a slightly different form than the original model's equation proposed by Phan-Thien and Tanner (1977). In fact equation (2.5) is written as in the chosen software to conduct the simulations. The Newtonian constitutive equation is recovered from the PPT model by setting $\xi$=1 and $\lambda$=0.

#### *2.4.2.3 PTT parameters*

The rheology of two different polymers were characterized at Case Western Reserve University: PS 615 (Dow) and PMMA VS100 (Altuglas International Arkema Group). When processed to form a two-component multilayered materials PS 615/PMMA VS100 (Dow/Altuglas international Arkema Group) is considered experimentally as a good pair for layering. Dr Maia's group determined and measured parameters of each polymer using IRIS software and shear and extensional rheometers. They are characterized by a multimode viscoelastic PTT model. For each, 6 modes have been found. They can be found in Table 2.1.

| PMMA VS 100 | | | PS 615 | |
|---|---|---|---|---|
| $G_i$ (Pa) | λ (s) | | $G_i$ (Pa) | λ (s) |
| 4.20E+05 | 5.96E-05 | | 1.82E+05 | 3.14E-04 |
| 7.22E+04 | 3.24E-03 | | 7.40E+04 | 2.53E-03 |
| 1.51E+05 | 6.22E-04 | | 2.68E+04 | 1.26E-02 |
| 2.27E+04 | 1.36E-02 | | 7.11E+03 | 5.32E-02 |
| 3.08E+03 | 6.02E-02 | | 9.43E+02 | 2.33E-01 |
| 1.91E+01 | 7.85E-01 | | 3.62E+01 | 1.26E+00 |
| | | | | |
| ξ | ε | | ξ | ε |
| 0.546 | 0.49 | | 0.51 | 0.072 |

**Table 2.1.** Measured parameters of PMMA VS100 and PS 615 at 230°C.

The parameters used by POLYFLOW are slightly different than those generated by the IRIS model but are easy to connect. The parameter $G_i$ is not used in the POLYFLOW model, but rather a viscosity parameter $\eta_i$, which is related to $G_i$ by the expression

$$\eta_i = G_i \lambda_i . \tag{2.12}$$

The useful parameters for the PTT models are then given in Table 2.2. The highlighted data in Table 2.2 are used for the PTT constitutive equation in Ansys POLYFLOW. However, only two modes are being used in order to spare CPU memory and time (speed and efficiency purposes) in the simulations presented in the next chapters. The viscosity of these two modes ($\eta_1$ and $\eta_2$) has been highlighted in orange in Table 2.2. As explained above the purely viscous component ($\eta_2$) is added for stability reasons and corresponds to the fastest relaxation time (Ansys POLYFLOW 12.1 user's guide 2009). We therefore have the following inputs in Ansys POLYFLOW problem setup:

| PMMA VS 100 | | | PS 615 | |
|---|---|---|---|---|
| **λ (s)** | **η (Pa.s)** | | **λ (s)** | **η (Pa.s)** |
| 5.96E-05 | 2.50E+01 | | 3.14E-04 | 5.71E+01 |
| 3.24E-03 | 2.34E+02 | | 2.53E-03 | 1.87E+02 |
| 6.22E-04 | 9.36E+01 | | 1.26E-02 | 3.38E+02 |
| 1.36E-02 | 3.09E+02 | | 5.32E-02 | 3.79E+02 |
| 6.02E-02 | 1.85E+02 | | 2.33E-01 | 2.19E+02 |
| 7.85E-01 | 1.50E+01 | | 1.26E+00 | 4.54E+01 |
| | | | | |
| **ξ** | **ε** | | **ξ** | **ε** |
| 0.546 | 0.49 | | 0.51 | 0.072 |

**Table 2.2.** Multimode PTT parameters to model PMMAVS100 and PS615 in Ansys POLYFLOW.

| | POLYFLOW variable name | PMMAVS100 | PS615 |
|---|---|---|---|
| $\eta_r$ (Pa.s) | ratio | 39.99 | 102.47 |
| η (Pa.s) | visc | 0.63 | 0.56 |
| ξ | xi | 0.546 | 0.51 |
| ε | eps | 0.49 | 0.072 |
| λ (s) | trelax | 0.785 | 1.26 |

**Table 2.3.** Material parameters in Ansys POLYFLOW at 230$^{o}$C

## 2.5 SUMMARY

The geometries of the feedblock and two multiplier dies have been presented as well as the equations of motion, the constitutive equations governing the flow of the polymers inside those channels. The Phan-Thien Tanner (Phan-Thien and Tanner 1977) model has been chosen because it gives the best fit of the experimental rheological data of typical materials. Two polymers currently used in the discussed multilayering process

have been characterized by Maia's group and their parameters (relaxation time, viscosity, elongation and elasticity) have been presented.

Using this model and these parameters, simulations have been run in order to simulate the behavior in the feedblock (chapter 3) and multiplier dies (chapter 4). They are used to track the interface and predict instabilities and degrees of encapsulation as a function of process parameters, primarily the flow rates and rheology of the polymers. Specifically, we will look at the velocity profiles, the position of the interface, the degree of encapsulation and the seconday flows with regards to the pair of polymers.

# Chapter 3: Simulations of the Feedblock

## 3.1 Introduction

This chapter presents the results of the simulations of the flow polymers inside the feedblock, including numerical issues specific to the feedblcok. Simulations of Newtonian fluids are conducted for the coextrusion of materials with different viscosity ratios to better understand the effect of viscosity on the shape and stability of the interface. Simulations are also done for non-Newtonian Phan-Thien-Tanner (PTT) fluids to understand the effects of elasticity on interface stability.

## 3.2 Simulation of the Feedblock

Figure 3.1 illustrates half of the feedblock in DesignModeler and the meshing of the domain. There are two planes of symmetry: one VW plane and one VX plane (see Figure 3.1 for coordinate planes). The simulations can be run with only a fourth of the geometry by specifying symmetry boundary conditions on these two planes. However, it is found that running on the half domain gives better results for tracking interface positions. The chosen half domain disregards the existence of the VX plane of symmetry.

a. b.

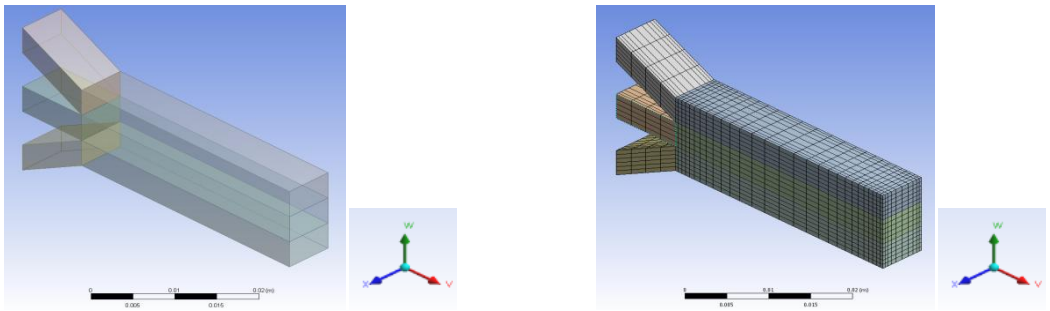

**Figure 3.1.** a) Idealization of half of the feedblock's geometry on DesignModeler; b) Mesh view of this same geometry. The flow is directed towards the positive V direction.

### 3.2.1 Boundary conditions

Five different types of boundary conditions can be distinguished (Table 3.1), and the surfaces of same boundary conditions are combined.

| 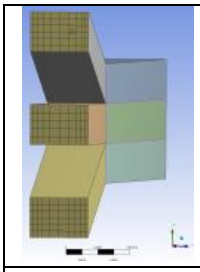 | 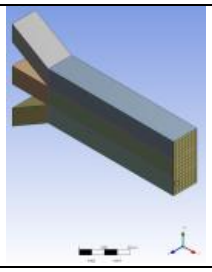 | 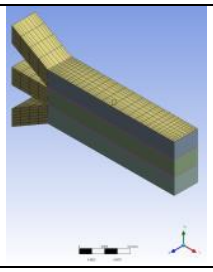 | 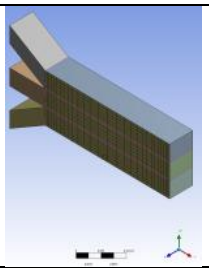 | 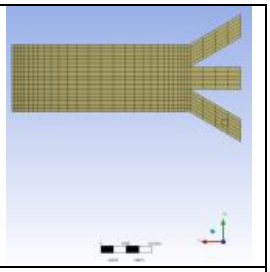 |
|---|---|---|---|---|
| Inputs | Outputs | No slip walls | Slipping wall | Plane of symmetry |

**Table 3.1.** Boundary conditions on the idealized feedblock's geometry.

*Inputs:* The top and bottom layers are fed with the same fluid at the same flow rate of $1.6 \times 10^{-7} m^3 s^{-1}$. The middle of inner fluid is fed at a slightly lower flow rate of $1.2 \times 10^{-7} m^3 s^{-1}$. The flow rates parameters are chosen according to typical experimental conditions (Figure 2.4)

*Outputs:* The outflow boundary condition is different according to the chosen constitutive model (Ansys POLYFLOW 12.1 user's guide 2009): a vanishing normal force and a vanishing tangential velocity when the PTT model is used; an outflow boundary condition for the Newtonian case.

*No slip boundaries:* The third boundary condition is simply a vanishing normal velocity and a vanishing tangential velocity or no-slip condition which is applied to solid walls in contact with a single fluid.

*Slipping wall:* For the wall on which the interfaces touch, a slip condition is applied. This is necessary to allow the interface positions to adjust downstream of their inception. A no slip boundary condition set on this side wall prevents the interface

between the layers to move freely. Per the POLYFLOW tutorial (Example 49 in Ansys POLYFLOW 12.1 Examples Manual 2009), a general Navier's law is used for the slip condition along this boundary condition. This consists of imposing simultaneously a zero normal velocity component and the following relationship between the shear force and the tangential relative velocity:

$$\mathbf{F} = -k\mathbf{v}_s. \tag{3.1}$$

As suggested in Polyflow user's guide (Ansys POLYFLOW 12.1 user's guide 2009), an evolution scheme on the parameter k is applied to help the convergence. An exponential type scheme is applied to guarantee a zero velocity equivalent (one per cent of the bulk velocity) at the wall:

$$k(S) = 20000\exp[3.5S] + 5000, \tag{3.2}$$

*S* is the evolution variable which varies from 0 to 1, therefore the parameter *k* varies from 5000 to 667309 $kg.s^{-1}$ (section 25-2 in Ansys POLYFLOW user's guide 2009).

*Plane of symmetry:* At the plane of symmetry along the center of flow the normal velocity and tangential forces are set to zero.

### 3.2.2 Simulation setup

Each layer is setup in Ansys Polydata separately and is considered as one domain (Ansys POLYFLOW 12.1 user's guide 2009; Ansys POLYFLOW 12.1 Examples Manual 2009) (Figure **3.2**). The interface boundary condition on the top and bottom surfaces of the middle domain is now setup as a *free moving interface*.

a. b. c.

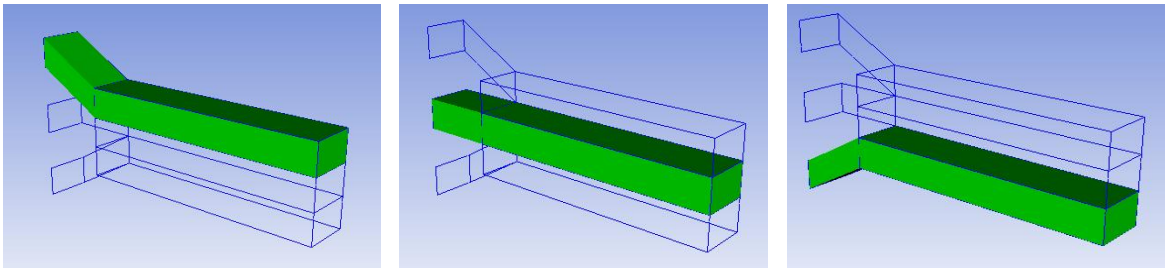

**Figure 3.2.** Domain selection in Ansys Polydata a) upper domain; b) middle domain; c) lower domain.

In the "material data" section of Polydata, the fluids' parameters are set and a model (PTT or Newtonian) is chosen. For the PTT model, the following evolution scheme is used on the relaxation parameter $\lambda$ in order again to avoid convergences difficulties:

$$f(S) = S \tag{3.3}$$

S is again the evolution parameter, varying from 0 to 1 (which makes $\lambda$ ranging from 0 to its true value) with an increment $dS$ set in the evolution setup. Thanks to the evolution scheme, the problem is first solved for the easier problem ($\lambda$=0) and gradually goes towards the solution of the true problem setup (section 25-2 in Ansys POLYFLOW user's guide 2009).

The PTT parameters are recalled in the model can be found in Table 3.1 below.

| | POLYFLOW variable name | PMMAVS100 | PS615 |
|---|---|---|---|
| $\eta_r$ (Pa.s) | ratio | 39.99 | 0.56 |
| $\eta$ (Pa.s) | visc | 0.63 | 102.47 |
| $\xi$ | xi | 0.51 | 0.51 |
| $\varepsilon$ | eps | 0.072 | 0.072 |
| $\lambda$ (s) | trelax | 0.785 | 1.26 |

**Table 3.2.** Material parameters in Ansys Polyflow at 230C

## 3.3 RESULTS

### 3.3.1 Newtonian simulations

#### *3.3.1.1 Influence of the viscosity ratio*

Simulations were first run for a pair of Newtonian fluids: fluid A of viscosity 10 Pa.s and fluid B of viscosity 100 Pa.s. They are extruded with the nominal flow rates given in Figure 2.4. As shown in Figure 3.3, the maximum velocity is not necessarily in the center of the channel. The maximum velocity is reached on the sides when the less viscous fluid is at the walls. This is surprising since this does not occur for two-dimensional flows. However, the three-dimensional nature of the flow and the roughly square full flow domain admit such a solution.

We can also notice the direction of curvature of the interface at the wall in Figure 3.3a and Figure 3.3b. The less viscous fluid covers more of the wall surface than the more viscous fluid as expected (Southern & Ballman 1973; Dooley 2002; Yue *et al.* 2008). The curvature of the interface is towards the more viscous material B in both cases.

Figure 3.4 illustrates this conclusion too. It features the position of the interface at the center and at the wall of the feedblock for the coextrusion of fluids of different viscosity ratio. The less viscous fluid wets more of the wall. This curvature very slightly increases with a bigger ratio. The interface is very much flat at the output of the feedblock. But it is interesting to note that, even for a viscosity ratio equal to 1 (extrusion 10/10/10 and 1000/1000/1000), a little curvature of the interface happens as well (the total height of the feedblock is 13.02 mm). This must be due to the difference of flow rates between the layers.

a.

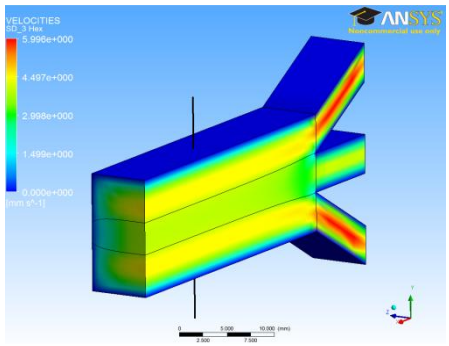

b.

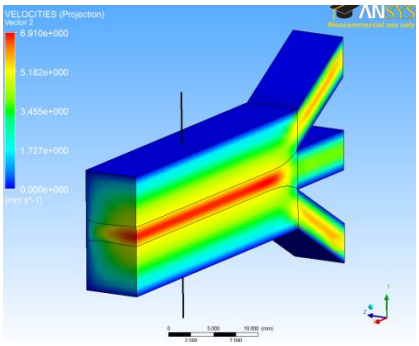

c

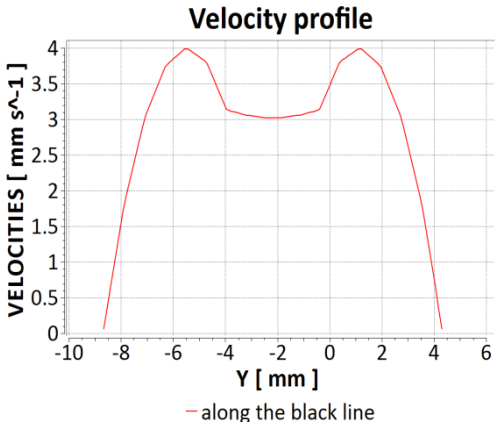


d.

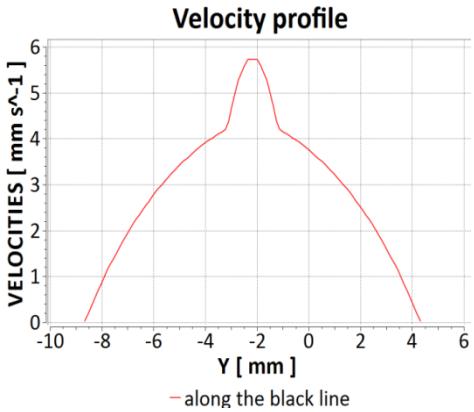


**Figure 3.3.** Velocity profile inside the feedblock domain and along the black vertical line. a) and c) refer to the ABA extrusion; b) and d) refer to the BAB extrusion. Viscosity of material A is 10 Pa.s and the viscosity of material B is 100 Pa.s.

Moreover, the thickness of the layers is better balanced when the lower viscosity fluid is along the wall. In fact the layer thickness is almost uniform in that case shown in Figure 3.3a as opposed to the much thinner inner layer in Figure 3.3b.

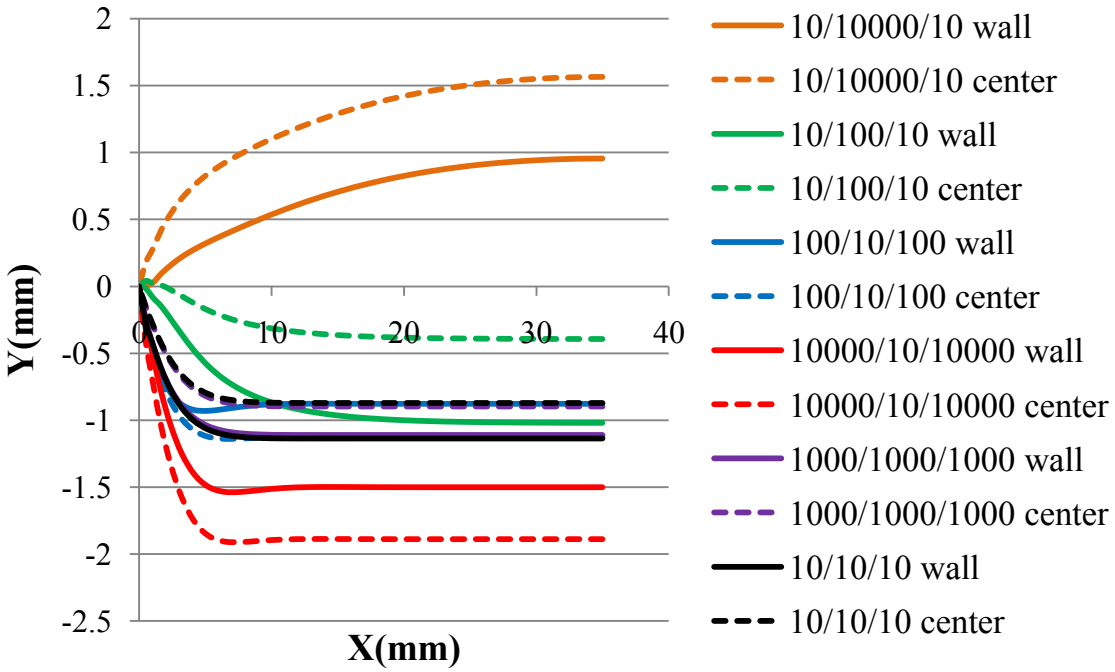


**Figure 3.4.** Interface position at the center and wall for different viscosities given in Poise. Note the total height of the feedblock is 13.02 mm.

The effect of the viscosity ratio on the interface inside the feedblock has also been studied in Figure 3.5. Simulations for viscosity ratios (viscosity of the top layer (in Pa.s) divided by the viscosity of the middle layer (in Pa.s)) from 1/1000 to 1000 have been conducted. The interfaces are far from pinching off. Plus, the length of the feedblock is sufficient to let the interface develop fully and become flat (Figure 3.5).

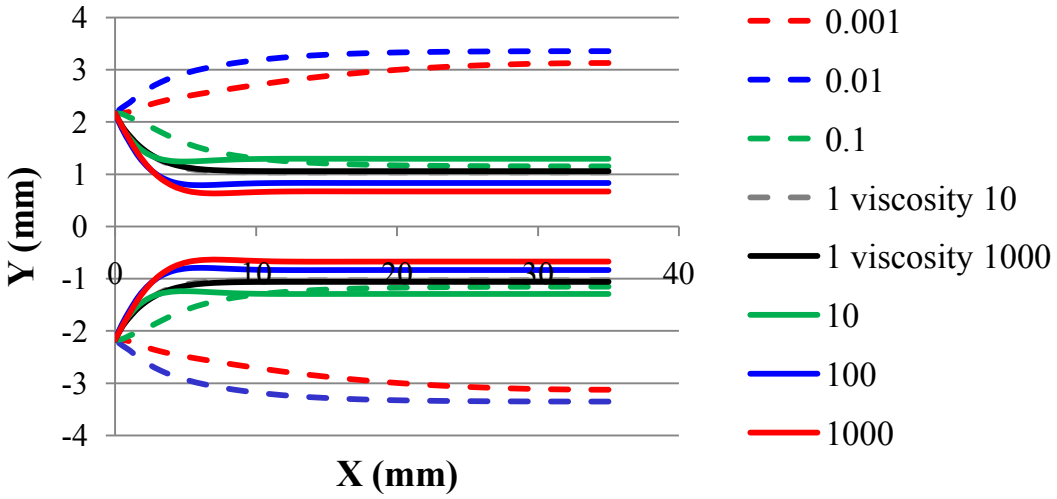


**Figure 3.5.** Downstream interface development for different viscosity ratio wall/center fluids. The viscosity ratios located on the left were as follows (in Pa.s): $10/10^4/10$; 10/1000/10; 10/100/10; 10/10/10; 1000/1000/1000; 100/10/100; $10^3/10/10^3$; $10^4/10/10^4$.

### *3.3.1.2 Newtonian equivalent to the true problem*

A preliminary model was built for the closest possible Newtonian fluid with comparable viscosity parameters to those characterizing the actual extruded polymers. The Newtonian fluids have been given the following viscosities: 39.99Pa.s for the Newtonian equivalent to PMMAVS100 and 102.47Pa.s for the equivalent PS615. The results are illustrated in Figure 3.6.

The velocity field, the position of the interface and the secondary flows are the focus of the results of the simulations. 3D contours of the velocity field have been created. Moreover, in order to study the secondary flows, we are plotting the planar streamlines (in red) and the projection of the velocity vectors on these planar cuts (in blue) amplified by a certain factor in order to be able to see the vectors.

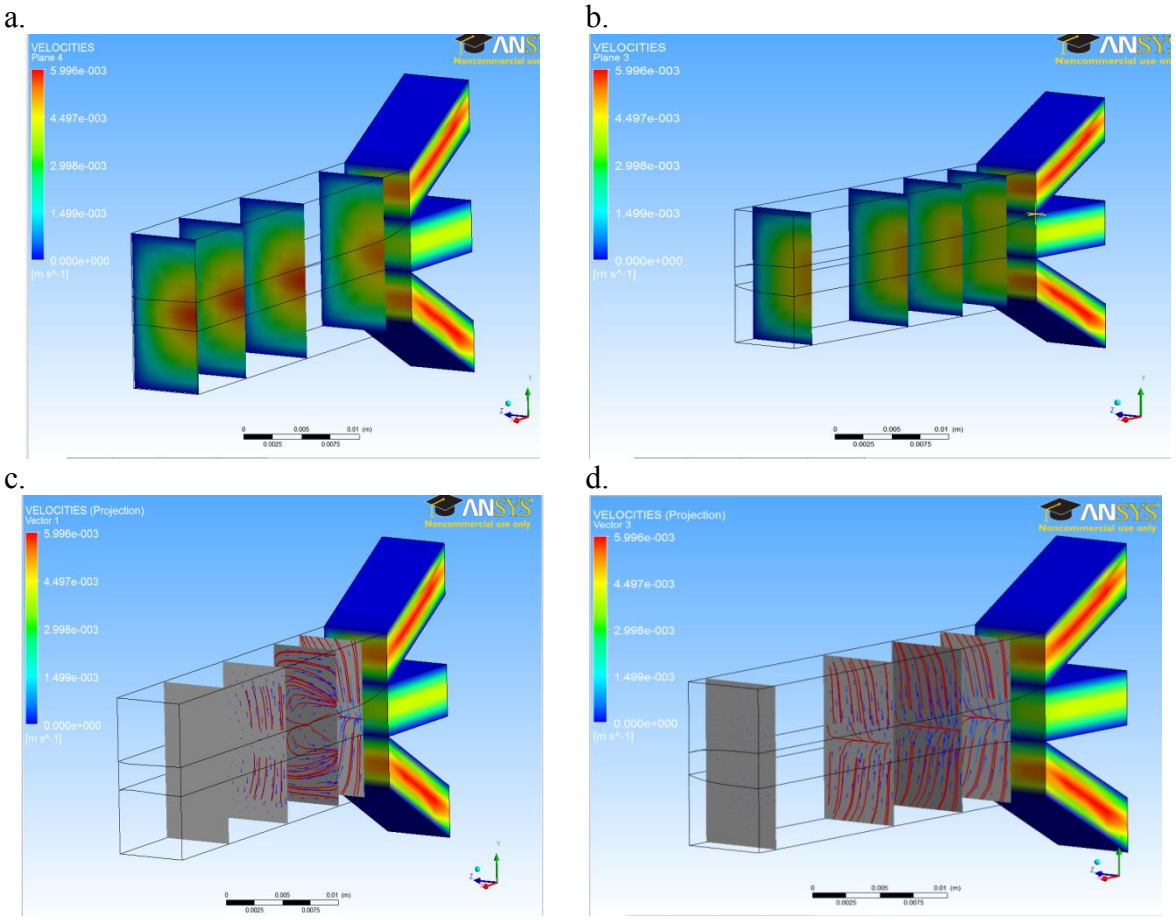


**Figure 3.6** a) Velocity field inside the feedblock domain for the coextrusion of the newtonian equivalent of PS/PMMA/PMMA; b) Velocity field inside the feedblock domain for the coextrusion of the newtonian equivalent of PMMA/PS/PMMA; c) four sections of the same flow as figure a) featuring the streamlines (in red) and the projection of the velocity vectors on these planes (in blue) amplified by a factor of 15 (section 1), 500 (section 2) and 10000 (section 3 and 4); d) four sections of the same flow as figure b) featuring the streamlines (in red) and the projection of the velocity vectors on these planes (in blue) amplified by a factor of 15 (section 1), 80 (section 2), 800 (section 3) and 10000 (section 4).

We can observe that the interface is relatively flat at the output: the viscosity ratio is only equal to three and there is no encapsulation (Southern & Ballman 1973; Dooley 2002; Yue *et al.* 2008). In both Figure 3.6c and Figure 3.6d, the arrows first points downwards of relatively important amplitude. This is due to the angle set between the

input channels of the feedblock. A weak cross flow is therefore created. It then decreases as the fluid flows downstream to eventually totally vanish at the output of the domain as it should. In fact when a purely viscous fluid flows in a straight channel, there is no flow perpendicular to the main flow (Tanoue *et al.* 2006). After being fully developed, no secondary flow is developed in the Newtonian cases (Figure 3.6) as expected.

### 3.3.2 PTT simulations

#### *3.3.2.1 Simulations matching the experiments*

The simulations of the polymers (modeled by the PTT model) show different results compared to the Newtonian cases (Figure 3.7 and Figure 3.8). Figure 3.7 shows the results (velocity field, interface position and streamlines (in red) and projected velocity vectors on the sections (in blue)) of the simulation of the coextrusion PS615/PMMAVS100/PS615 characterized by the PTT model while Figure 3.8 shows the simulation of the coextrusion PMMAVS100/PS615/PMMAVS100 also characterized by the PTT model.

A secondary flow in the plane normal to the primary direction of flow develops. As opposed to the Newtonian case, these secondary flows do not vanish at the outlet and affects the flatness of the interface. It is not as flat as in the Newtonian flows but still very far from encapsulation despite these secondary flows. Moreover, the curvature in Figure 3.8 is slightly toward the less viscous fluid at the output. This is the opposite behavior of what has been observed for Newtonian fluids in Figure 3.6b and Figure 3.6d. The elastic behavior of the fluids must be responsible for this change. Further simulations have been run to verify this hypothesis.

a. b.

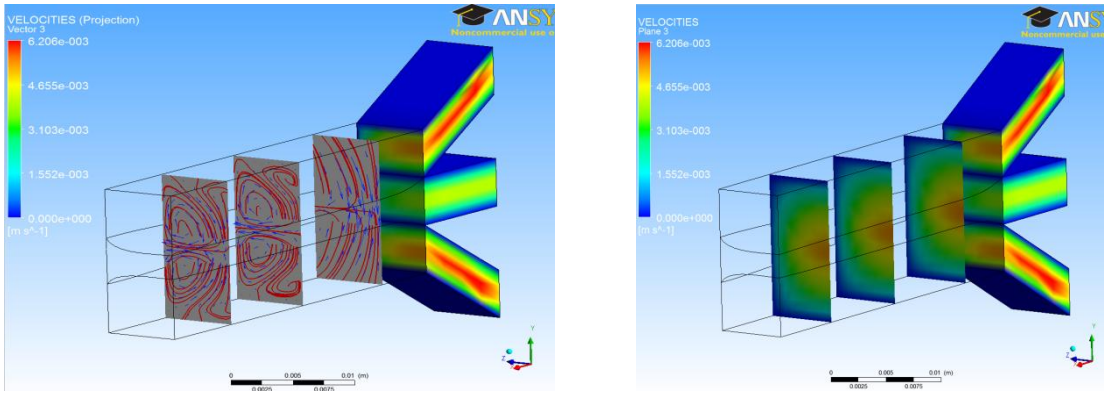


**Figure 3.7** a) Sections of the velocity field inside the feedblock domain for the coextrusion of PS615/PMMAVS100/PS615; b) three sections of the same flow as figure a) featuring the streamlines (in red) and the projection of the velocity vectors on these planes (in blue) amplified by a factor of 55 (section 1), 150 (sections 2 and 3).

a. b.

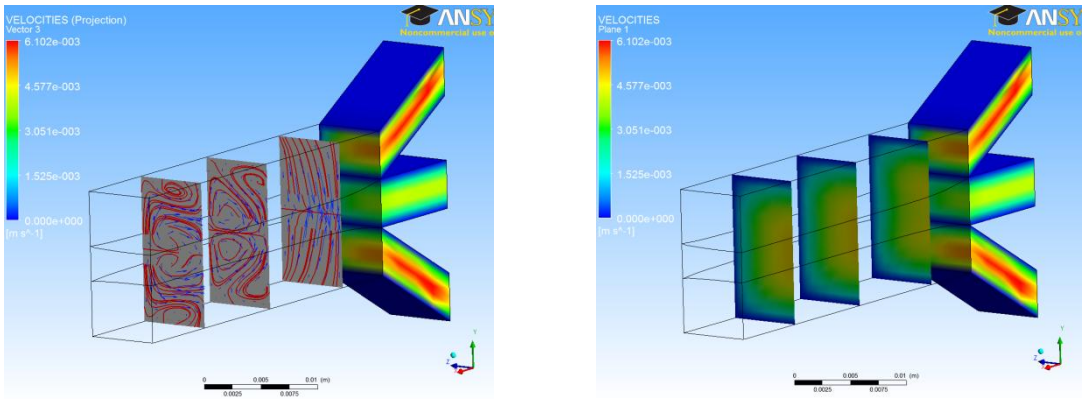


**Figure 3.8** a) Sections of the velocity field inside the feedblock domain for the coextrusion of PMMAVS100/PS615/PMMAVS100; b) three sections of the same flow as figure a) featuring the streamlines (in red) and the projection of the velocity vectors on these planes (in blue) amplified by a factor of 45 (section 1), 400 (sections 2, 3 and 4).

Finally, it is interesting to notice how the characterization of the fluid affects the position of the interface (Figure 3.9). In the PTT case, there is an inflection in the interface's position and the length of the feedblock does not seem long enough for the

interface to settle at a certain height as opposed to the Newtonian case where it settles down quickly. This inflection is probably due to the development of secondary flows. They don't vanish as the fluid moves downstream for PTT fluids as they do for Newtonian fluids.

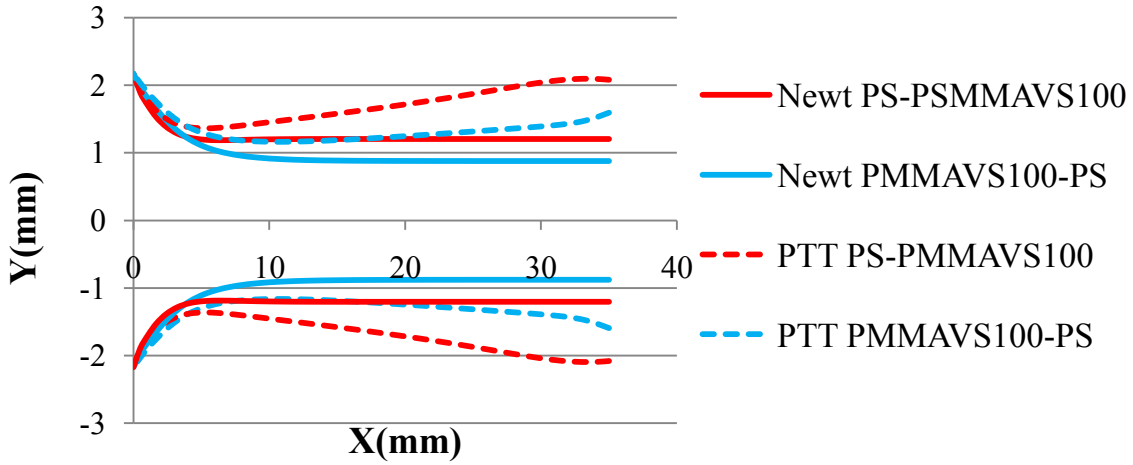


**Figure 3.9.** XY interface at the wall for pairs of polymers in their Newtonian form and their PTT form.

### *3.3.2.2 Further simulations*

Studies show that second normal stress difference must contribute to the development of the secondary flows (Xue *et al.* 1995, Tanoue *et al.* 2006) and that the importance of these secondary flows is directly related to the elasticity.

Figure 3.10 illustrates the extrusion at the wall of a more elastic material than the previous PMMAVS100 at the wall and PS615 in the middle. This new polymer (PMMAVS100*) is three times more elastic. The relaxation time is now of 2.36s. The interface stays really stable and the curvature of the interface has slightly increased compared to Figure 3.8. It is still towards the less viscous fluid after 25mm of the die as the secondary flows are more vortical and whirling than the ones observed in Figure 3.8.

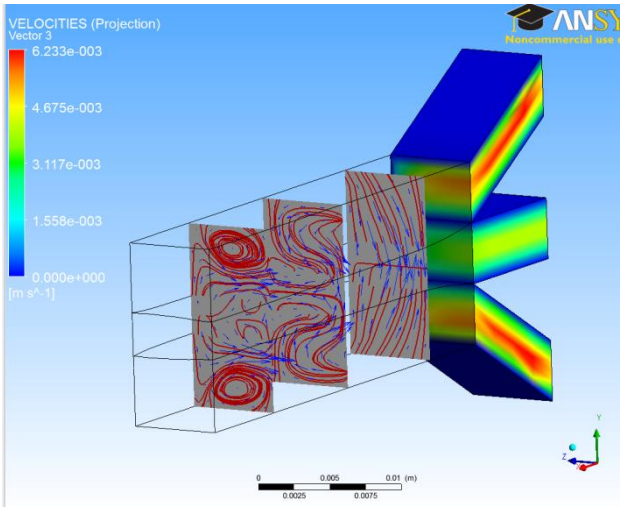


**Figure 3.10.** Three sections of the coextrusion of PMMAVS100*/PS/ PMMAVS100* featuring the streamlines (in red) and the projection of the velocity vectors on these planes (in blue) amplified by a factor of 45 (section 1), 400 (sections 2, 3 and 4). PMMAVS100* is a polymer with the same parameters as PMMAVS100 but its elasticity parameter is three times bigger.

Figure 3.11 illustrates the coextrusion of a less viscous material than the previous PMMAVS100 at the wall and PS615 in the middle. This new polymer (PMMAVS100**) is ten times less viscous. The viscosity parameter is now of 3.99 Pa.s therefore the viscosity ratio is 25.7. As discussed in 3.3.1.1, this viscosity ratio would not have created this almost total encapsulation if we had extruded Newtonian fluids.

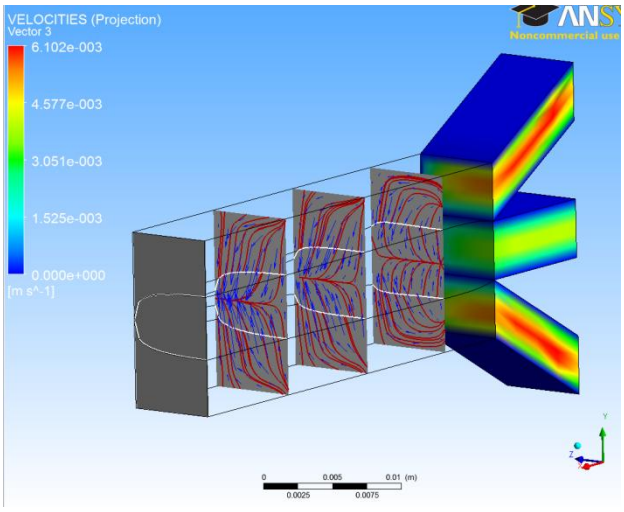


**Figure 3.11.** Three sections of the coextrusion of PMMAVS100**/PS/ PMMAVS100** featuring the streamlines (in red) and the projection of the velocity vectors on these planes (in blue) amplified by a factor of 45 (section 1), 400 (sections 2, 3). The last plane shows how close to the pinch off the interface is. PMMAVS100** is a polymer with the same parameters as PMMAVS100 but its viscosity parameter is ten times smaller.

To understand better what is causing this almost total encapsulation, we have run the same simulation as in Figure 3.11 but turning off the elasticity parameter of one or the other layer. Figure 3.12 illustrates the coextrusion of the Newtonian equivalent fluid to PMMAVS100** (i.e. a Newtonian fluid of viscosity 3.99 Pa.s) at the walls with a PS615 middle layer described with the PTT model, whereas Figure 3.13 shows the coextrusion of PMMAVS100** at the wall modeled by the PTT equations and the Newtonian equivalent fluid to PS615 (i.e. a Newtonian fluid of viscosity 102.46) in the middle.

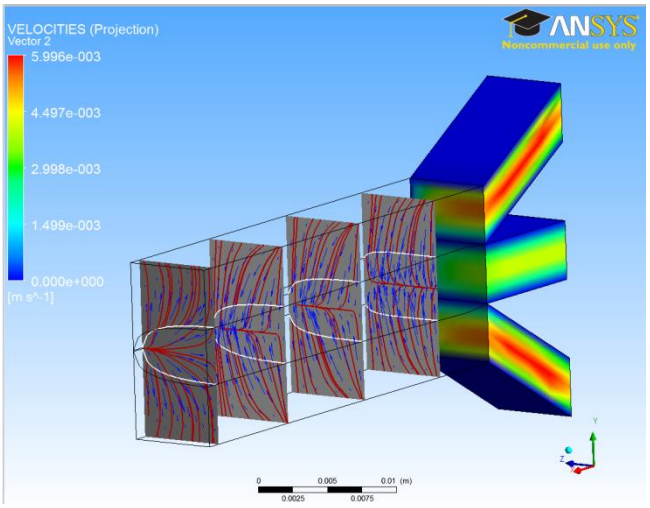


**Figure 3.12.** Four sections of the coextrusion of the Newtonian equivalent of PMMAVS100** at the walls (i.e. a Newtonian fluid of viscosity 3.99 Pa.s) with PS615 in the middle featuring the streamlines (in red) and the projection of the velocity vectors on these planes (in blue) amplified by a factor of 75 (sections 1 and 2), 150 (sections 3 and 4).

We can see that turning off the elasticity of the top and bottom layers does not affect the shape of the interface. It is still very close to the total encapsulation (Figure 3.12). However, turning off the elasticity of the middle layers seems to stabilize the interface (Figure 3.13). It is also to note that the curvature is again the opposite of what the viscosity ratio would predict: the less viscous fluid tends to encapsulate the more viscous fluid (cf section 1.3.2.2). On the contrary, although PS615 has a viscosity parameter three times bigger than the viscosity of the Newtonian fluid on top and bottom, the middle layer of PS615 wets more of the wall.

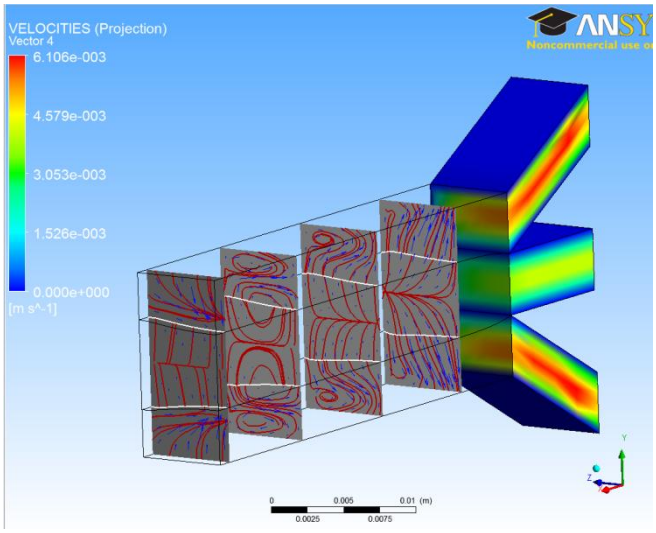


**Figure 3.13.** Four sections of the coextrusion of the Newtonian equivalent of PS615 in the middle (i.e. a Newtonian fluid of viscosity 102.47 Pa.s) with PMMAVS100** at the walls featuring the streamlines (in red) and the projection of the velocity vectors on these planes (in blue) amplified by a factor of 100(sections 1, 2 and 3), 70 (section 4).

These simulations show the clear influence of the elasticity parameter in the coextrusion of polymers, especially the elasticity parameter of the middle layer versus the viscosity parameter of the top and bottom layers. We can reasonably conclude that it is preferable to extrude the less viscous material at the walls and the less elastic material in the middle.

## 3.4 CONCLUSIONS

We found that the interface stays relatively flat for fluids characterized by the Newtonian model. But it is better to extrude with the less viscous fluid at the wall so that uniform layer thicknesses are achieved at the output.

We have conducted simulations inside the feedblock for comparable Newtonian and PTT fluids that showed that secondary flows occur in both cases but don't vanish for the non-Newtonian fluids. Whereas in the Newtonian case, the fully developed profile and the constant height value of the interface are reached quickly after the merging of the

independent inputs, the non vanishing secondary flows prevents it from happening for the PTT case. But the interface position does not move much and no encapsulation occurs.

Simulations of layers of Newtonian fluids have been run for different viscosity ratios. No encapsulation is happening regardless of the ratio value. However, although the simulations with Newtonian fluids led to the conclusion that the viscosity ratio is not the main cause of the instability of the interface, further simulations with the PTT model showed the complex combination between viscosity and elastic parameters of both materials. Secondary flows promoted by the elastic behavior of the polymer can compensate the effect of the viscosity ratio in certain cases and a viscosity ratio value of 25 is sufficient to get an almost total encapsulation.

# Chapter 4: Simulations of Multiplier Dies

## 4.1 Introduction

This chapter presents the setup and the results of the simulations that have been conducted with Ansys POLYFLOW (Appendix) for the multiplier geometries presented in chapter 2. Simulations for the polymer pairs PS 615 and PMMA VS100 have been run for the current and the new multiplier geometries in order to study the behavior of the interfaces between the polymers and also the impact of the geometry of the multiplier itself on the flow parameters such as pressure drop and secondary flows.

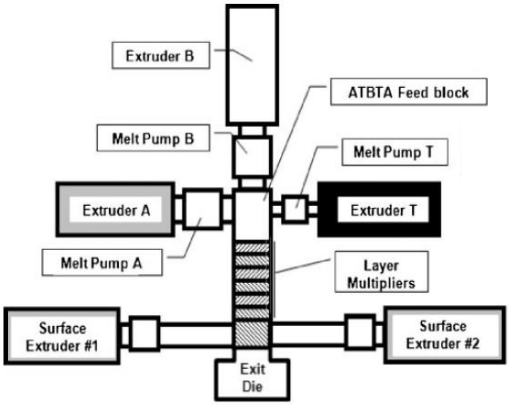


**Figure 4.1.** Overall schematic of the multilayering process presented in this thesis from Ponting *et al.* (2010a).

Recall, the function of the multiplier is to cut, split and stack the polymer layers on top of each other (Figure 4.2).

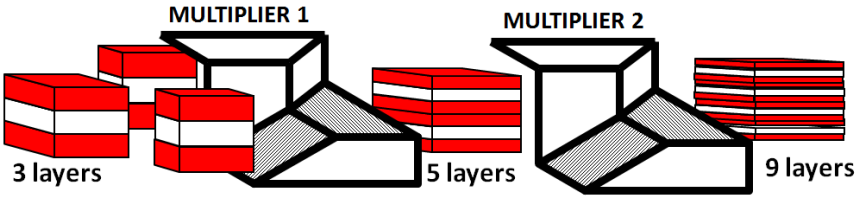


**Figure 4.2.** Schematic illustration of two mulitpliers for a two-component material.

## 4.2 BOUNDARY CONDITIONS

Three layers enter a multiplier. However, since the outflow of the feedblock is vertically split in two, the flow rates in the multiplier are half that in the feedblock. Therefore the top and bottom layers enter at a flow rate of $8.0 \times 10^{-8}$ $m^3$ $s^{-1}$ and the middle layer has a flow rate of $6.0 \times 10^{-8}$ $m^3$ $s^{-1}$.

a. b.

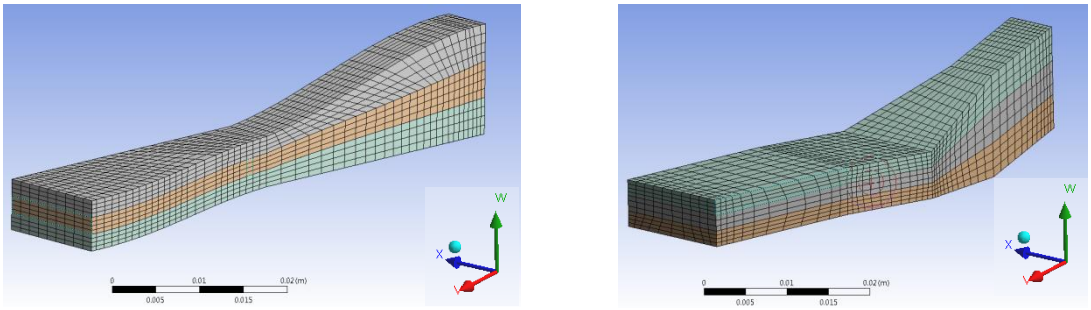

**Figure 4.3**. Mesh view of the multiplier dies. a) current multiplier design b) new multiplier design. The flow is directed towards the positive V direction.

Neither of these two geometries has a plane of symmetry. We therefore cannot reduce the computational domain as was done for the feedblock. This increases the computational time compared to the feedblock calculations considerably. Boundary conditions are comparable to those presented for the feedblock in 3.2.1 as follows: setting of inlet and outlet conditions, no slip on the upper and lower walls; slip conditions on the side walls along which the interface moves. The meshing of these domains is similar to the one in the previous chapter, as well as the boundary conditions, the evolution schemes and the setup (section 3.2.2) (Figure 4.3).

## 4.3 RESULTS

The velocity profiles of the current design and new design have been studied as well as the streamlines (red lines) of the flow and the projection of the velocity vectors on

planar sections (vectors in blue). The latter are amplified by a factor (specified in the caption) in order to be able to see the vectors on the pictures.

### 4.3.1 Current multiplier

Figure 4.4 illustrates the results of the simulation of the flow of a three layered PS615/PMMAVS100/PS615 material whereas Figure 4.5 shows the results for PMMAVS100/PS615/PMMAVS100 both in the current multiplier. The polymers are described by the PTT model with the parameters given in Table 2.3. Results show the velocity field as well as the shape of the interface and feature the planar streamlines (in red) and the projection on the plane of the velocity vectors (in blue) amplified by a factor given in the figure's caption.

This current geometry is characterized by the fact that it does not maintain a constant cross-sectional area normal to the main flow direction throughout the multiplier (as opposed to the new geometry). The flow is then more focused at the narrowest part and the velocity field is maximum at this section (Figure 4.4a and Figure 4.5a). The streamlines are as expected: the arrows in Figure 4.4b and Figure 4.5b point first downwards and then on the wider side of the domain following the curves of the geometry.

a.

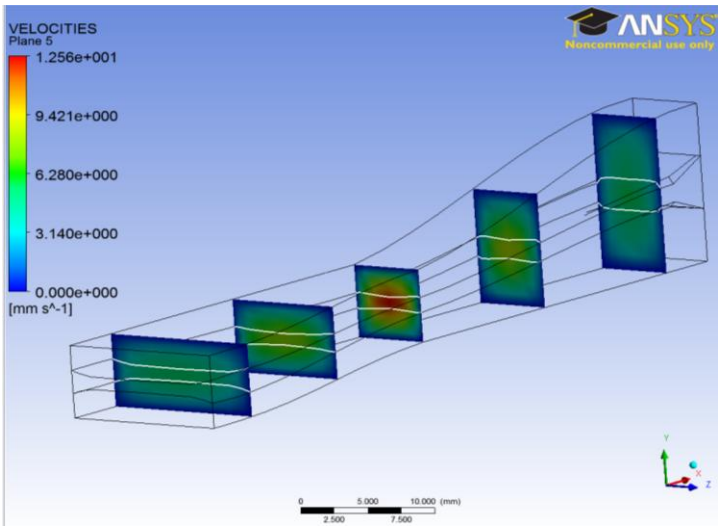


b.

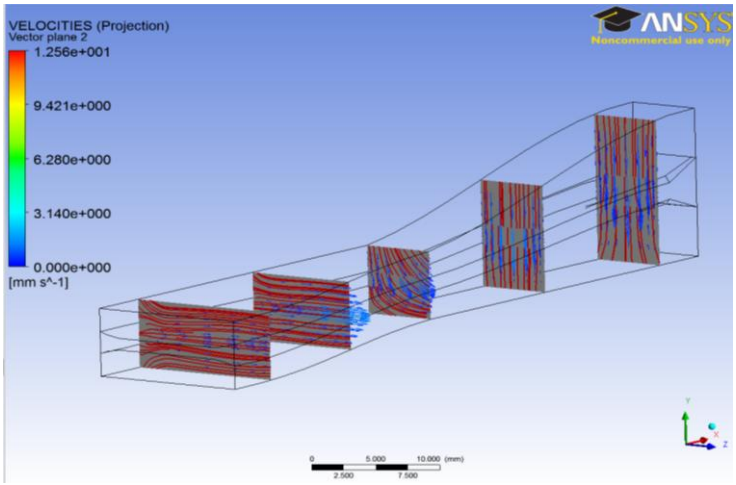


**Figure 4.4.** a)Velocity field inside the current multiplier domain for the coextrusion of PS615/PMMAVS100/PS615 modeled by the PTT constitutive equations; b) five sections of the same flow as figure a) featuring the streamlines (in red) and the projection of the velocity vectors on these planes (in blue) amplified by a factor of 25 (section 1), 10 (other sections).

Even though these secondary flows are quite strong, there is no encapsulation. However, as shown in Figure 4.5a, the interfaces are getting to the point that a lens of the interior fluid might be formed from the pinching off at the edges. The less viscous fluid

wets more of the wall surface than the more viscous fluid as expected from the simulations on the feedblock.

a.

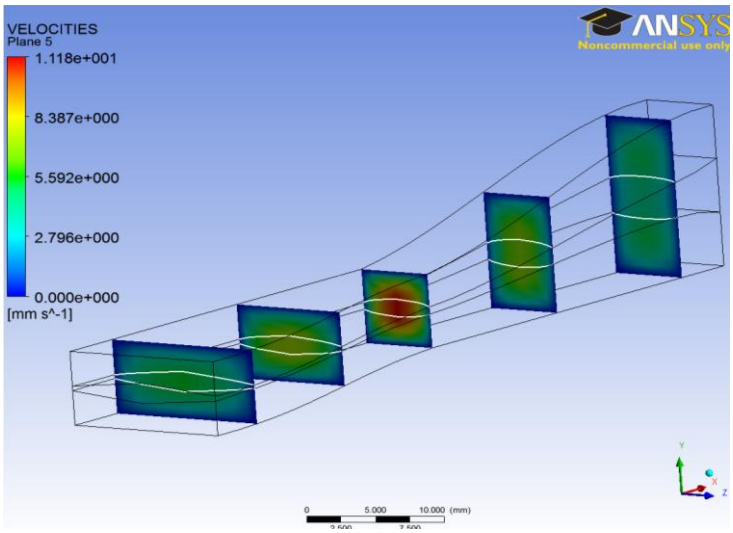


b.

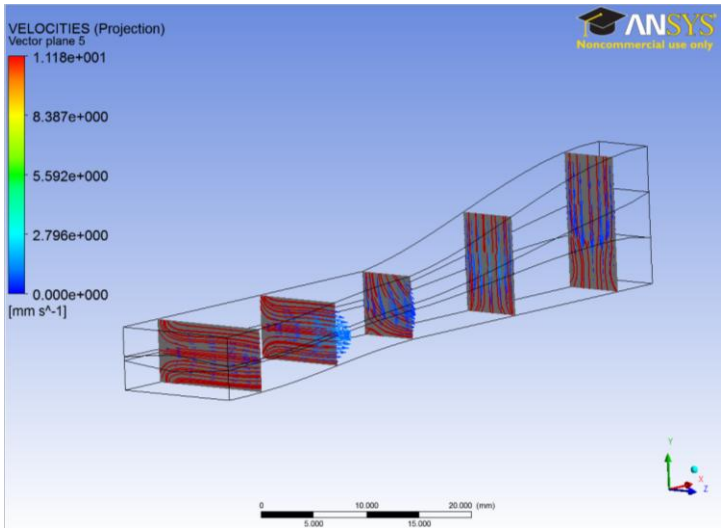


**Figure 4.5.** a)Velocity field inside the current multiplier domain for the coextrusion of PMMAVS100/PS615/ PMMAVS100 modeled by the PTT constitutive equations; b) five sections of the same flow as figure a) featuring the streamlines (in red) and the projection of the velocity vectors on these planes (in blue) amplified by a factor of 25 (section 1), 10 (other sections).

### 4.3.2 New multiplier

Figure 4.6 illustrates the results of the simulation of the flow of the three layers PMMAVS100/PS615/PMMAVS100 material in the new multiplier. The polymers are described by the PTT model with the parameters given in 2.3. Results show the velocity field as well as the shape of the interface and feature the planar streamlines (in red) and the projection on the plane of the velocity vectors (in blue) amplified by a factor given in the figure's caption.

This new geometry maintains a near constant cross-sectional area in the plane perpendicular to the main flow throughout the domain (as opposed to the current geometry). The velocity field of the flow is more uniform (Figure 4.6a) as the fluid moves downstream. However, the streamlines are more complicated. The arrows in Figure 4.4b point first downwards and then on the wider side of the domain following the direction of the flow and the geometry.

These secondary flows are quite strong, and the coextrusion is very close to the total encapsulation (even closer than in Figure 4.5a) as we can see the interfaces are almost pinching off to form a lense of the interior fluid.

The simulation with polystyrene on top and bottom of the domain (PTT model PS615/PMMAVS100/PS615) failed, apparently because the top interface ends up merging with the bottom interface, pushing the less viscous fluid (PMMA VS100) along the wall. The simulation currently cannot handle the merging of interfaces. The same simulation with a reduction of elasticity by a factor of two for both fluids has not reached convergence either.

a.

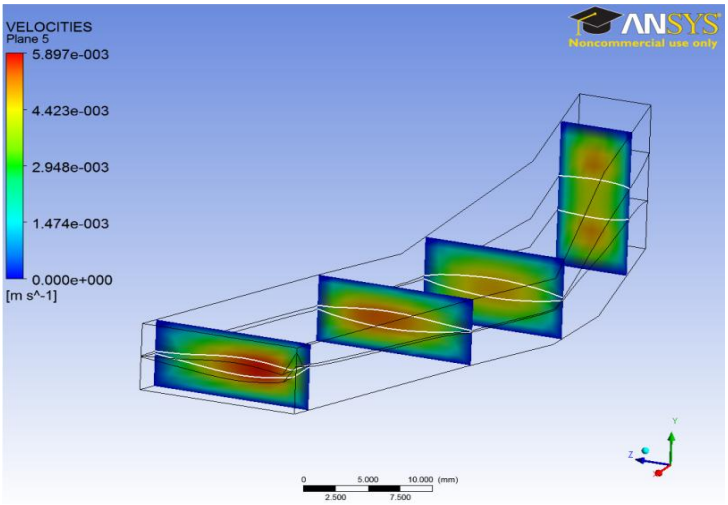


b.

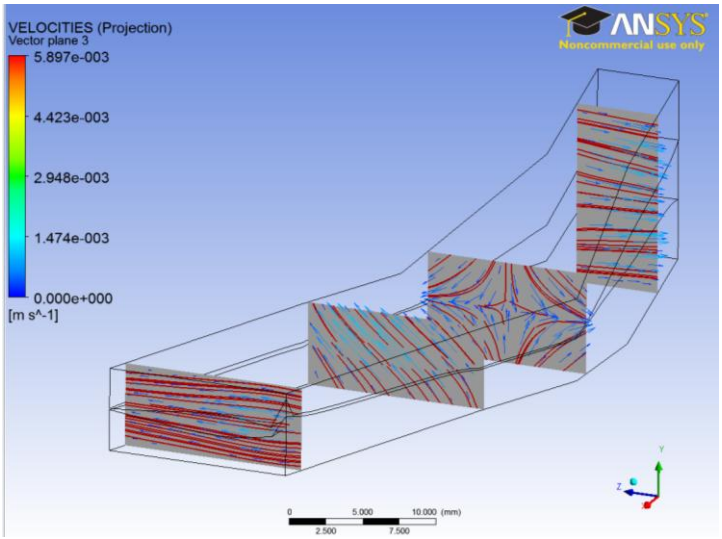


**Figure 4.6.** a)Velocity field inside the new multiplier domain for the coextrusion of PMMAVS100/PS615/ PMMAVS100 modeled by the PTT constitutive equations; b) four sections of the same flow as figure a) featuring the streamlines (in red) and the projection of the velocity vectors on these planes (in blue) amplified by a factor of 8 (section 1) and 5 (other sections).

Figure 4.7 illustrates the coextrusion of Newtonian fluids of viscosity ratio equal to the viscosity ratio between PS615 and PMMAVS100. The more viscous fluid is at the

walls and as opposed to the PTT case, the simulation has been run successfully. The interface behaves very well and comes out almost perfectly flat.

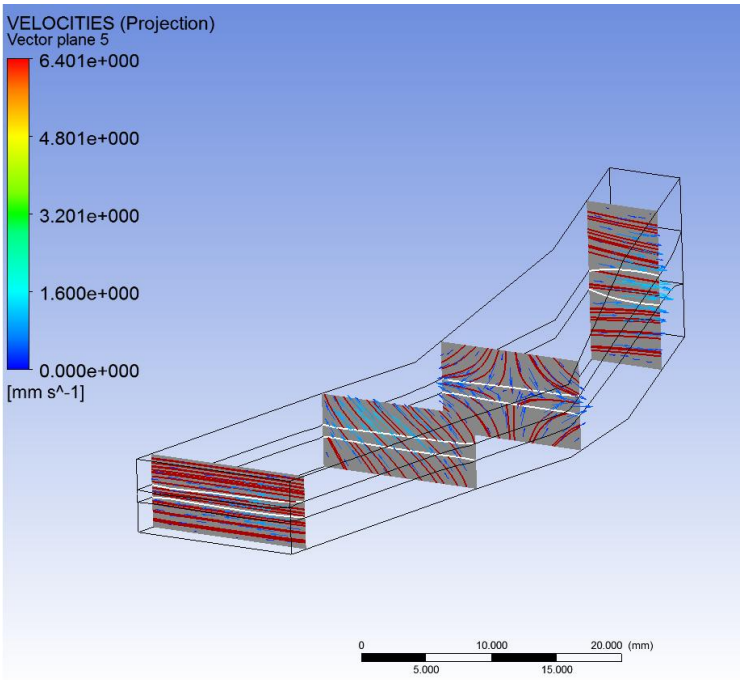


**Figure 4.7**. Four sections inside the new multiplier domain featuring the streamlines (in red) and the projection of the velocity vectors on these planes (in blue) amplified by a factor of 8 (section 1) and 5 (other sections) for the coextrusion of Newtonian fluids of viscosity 100/45/100 (Pa.s).

These results seem to confirm the conclusion made in chapter 3. The interface behavior is highly dependent on the elasticity parameter associated to the viscosity parameter. This combination seems even more important for this new multiplier as the interface behaves really well inside the current multiplier die (Figure 4.4).

### 4.3.3 Discussion

It is interesting to note how the geometry impacts the curvature of the interface. The interfaces in the coextrusion of PMMAVS100/PS615/PMMAVS100 are twice as

close from pinching off in the new design as they are in the current one. A closer look to the velocity field on the YZ plane section shows an opposite behavior: the projected velocity is twice as small in absolute value in the new multiplier as in the current multiplier. In fact, the maximum velocity reaches 11.18 $mm.s^{-1}$ in the current multiplier whereas it reaches only 5.90 $mm.s^{-1}$ in the new multiplier. Given these data, it appears surprising to find stronger secondary flows in the new design since they are generally scaled with the magnitude of the main flow. The secondary flows, causing the pinching off, must therefore be influenced by the geometry of the die. The second part of the new multiplier die that spreads horizontally the flow on a short length must be the reason of these stronger secondary flows. In fact, this expansion occurs throughout the whole length of the current die in which the secondary flows are smaller. This hypothesis is supported by the failure of simulating the coextrusion of PS615/PMMAVS100/PS615 inside the new multiplier die as opposed to the success of the Newtonian equivalent simulation.

### 4.3.4 Pressure drop in current and new multiplier

The new multiplier maintains near constant cross- sectional area s throughout the channel as opposed to the current multiplier that follows a smooth curve from the same input section to the same output section. Therefore, the new design reduces the pressure that is necessary to make the fluids flow into the channel. Figure 4.8 illustrates the pressure drop between the input and the output of the multiplier for a single fluid flowing through the current or the new die. This fluid has been characterized with either Newtonian or PTT constitutive equations. It can be seen that the new design reduces the pressure drop especially for higher flow rate. The same conclusions can be drawn from

Figure 4.9 illustrating the pressure drop for the extrusion of the three layered material PMMAVS100/PS615/PMMAVS100.

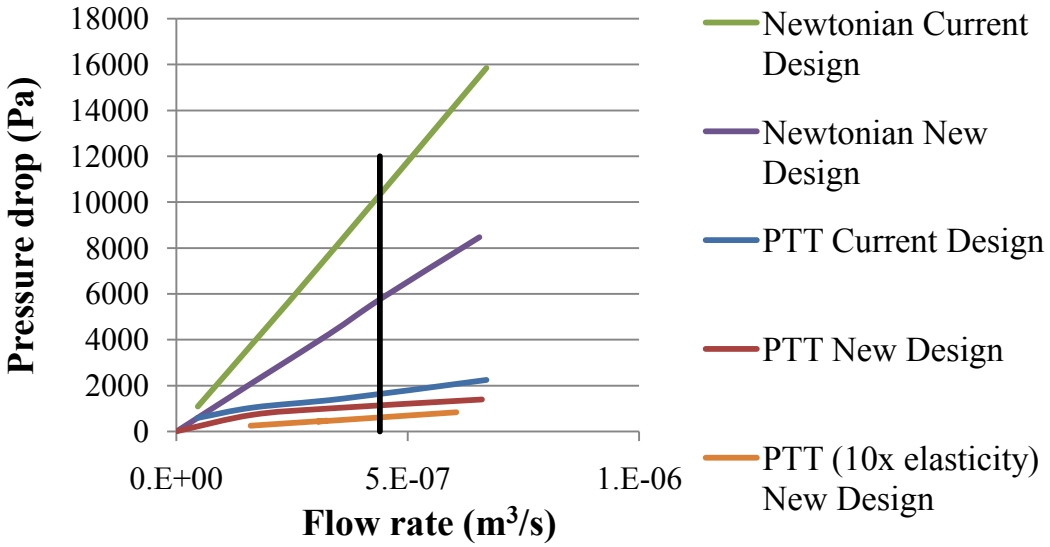


**Figure 4.8.** New Multiplier Design Reduces the Pressure Drop (single fluid). The black line is set at the nominal flow rate (4.4 x $10^{-7}$ $m^3.s^{-1}$).

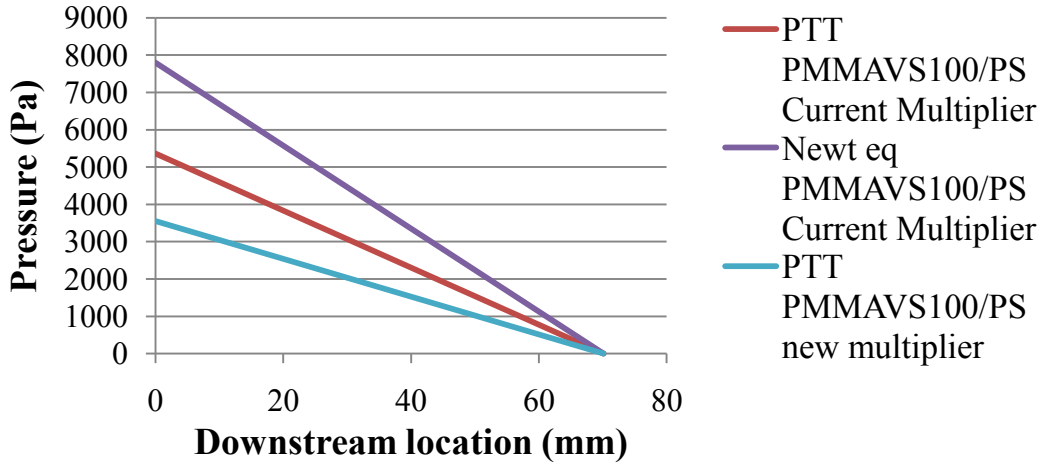


**Figure 4.9.** New Multiplier Design Reduces the Pressure Drop for the coextrusion of PMMAVS100/PS615/PMMAVS100

The experiments done by the Maia's group on the pressure drop shows that the pressure drop in the new multiplier design is around half the pressure drop measured in the current multiplier design. Our simulations are consistent with these findings. A minimized pressure drop means that less energy is needed to make the same product and a better efficiency.

## 4.4 CONCLUSIONS

Simulations of three layered polymer fluids described with the PTT model have been run in both current and new geometries. We found that the current geometry allows the multiplication of both pairs of polymers whereas the new geometry allows only the extrusion of the pair PMMAVS100/PS615/PMMAVS100.

The new multiplier design clearly decreases the pressure drop required to extrude the materials for any kind of fluid (Newtonian, non-Newtonian or very elastic) compared to the current multiplier design. This is due to the fact that it keeps the section of the multiplier rather constant. But this latter characteristic implies a very rapid planar extension to switch from a vertical section to a horizontal one. This creates stronger secondary flows that must deteriorate the quality of the layers and must be responsible for the incapacity of simulating the PS615/PMMAVS100/PS615 extrusion. This shows a strong interdependence between elasticity and viscosity parameters especially in the new design. The geometry of the multiplier die has therefore clearly a very important part in the success in layering polymers.

# Chapter 5: Concluding remarks

## 5.1 CONTEXT

This thesis focused on a multilayering method developed at Case Western Reserve University and now in the Center for Layerd Polymer Systems (CLiPS). This process currently works only for few pairs of polymers including the pair PMMAVS100-PS615. This research was motivated by the need to improve this technique in order to expand the process window. In fact, very exciting applications are already in need of new multilayered materials. In order to be able to generalize this process, a better understanding of the fluid flows as a function of the fluid parameters is required.

## 5.2 SUMMARY

A computational model was developed to simulate the flows in the feedblock and in two different multiplier dies. Both Newtonian and non-Newtonian fluid flows have been studied. The constitutive equations of the non-Newtonian polymers have been described by the Phan-Thien-Tanner (PTT) model.

Based on these models, simulations were run. The interface position has been tracked and the velocity field has been studied as well as the streamlines and the secondary flows inside the simulated domains. Our simulations were mainly focused on the extrusion of the pair of polymers PMMAVS100 and PS615.

Specifically, for the feedblock, we analyzed the effects on the stability of the interfaces of both, the viscosity contrast between the layered materials for Newtonian fluids and of both their viscosity and elasticity for non-Newtonian fluids. For the multiplier dies, we studied the behavior of the interfaces for polymer pairs used in practice. We finally compared between the two multiplier designs the pressure drops

required for an extrusion. With these data, we were able to evaluate the current and the new multiplier designs.

## 5.3 CONCLUSIONS

From the simulations of Newtonian fluids, we have established that the viscosity ratio between the layered materials is not a limiting parameter and does not influence significantly the flatness of the interface in the feedblock. However, for the non-Newtonian case (PTT), we discovered that the elasticity and the viscosity parameters are closely interdependent. In fact the first is responsible for the development of secondary flows as the fluids move downstream that can counter the effects of a big enough viscosity ratio (cf. 3.3.2.2). We have also found that the interface between PTT fluids does not settle to a constant height. On the contrary, it shows a slight inflection that must be due to the non vanishing secondary flows promoted by the elastic behavior of the polymers.

The multiplier die seems more likely to fail keeping the materials correctly layered due to the smaller dimensions, the more complex geometry and the necessity of a compression of the flow. The new design has been thought to be a good alternative to the current one but it appears that the interface of the extrusion of the pair PS615/PMMAVS100 has merged. It is due to a bigger development of secondary flows resulting from the combination of the elastic and viscous behavior of the polymers. The new geometry seems to be more sensitive to this combination than the current one. However, we have found that trying to keep the area constant throughout the geometry of the multiplier die (new design) was very advantageous for the pressure drop required to

extrude the materials. In fact it reduces by almost a factor of two the pressure drop after comparing them in the current and the new multiplier die.

## 5.4 RECOMMENDED FUTURE WORK

If the viscosity ratio between the coextruded materials had almost no effect on the interface's position for the coextrusion of Newtonian fluids inside the feedblock, the shape of the interface is highly dependent on the combination of both the viscosity and the elasticity parameters for PTT fluids. A more extensive parameter study is needed to understand their interdependence and would be very helpful to confirm if it is better to promote the less elastic fluid in the middle layer and the less viscous fluid at the walls.

A special focus of future work should be put on the multiplier since the instabilities seem to be more likely to occur in it for the reasons explained above. Being able to run simulations for a succession of multiplier dies would also be very helpful to see how the layers are behaving when they become smaller and smaller. As for the feedblock, a parameter study varying the elasticity and the viscosity parameters is needed to better understand why the new design fails for the second pair of polymers.

Finally, Ansys POLYFLOW is not able to handle simulations when total encapsulation occurs. The computation crashes when the interfaces pinch off. It seems essential to find commercialsoftware or to create a code that can handle the merging of the interfaces in order to support the hypothesis we have made with regards to the position of the less viscous fluid in the coextrusion process.

Plus, a redesign of the multiplier seems necessary to be able to combine the best of both geometries. In fact the extrusion is very close to the total encapsulation in the new multiplier design as opposed to the current one and the pressure drop of extrusion has

decreased by almost a factor of two. Conducting simulations for a single fluid and testing if contractions or expansions of the die would be very valuable to determine the adjustments that must be made on the design of a new die.

# Appendix: Simulation software: ANSYS POLYFLOW

## A.1 INTRODUCTION

A study of commercial software was conducted for the simulations for this thesis. The chosen software had to meet several criteria. It must be able to model 2D and 3D flows with both Newtonian and non-Newtonian fluids and include heat transfer effects. After a careful examination of several products, Ansys POLYFLOW was selected.

## A.2 GETTING TO KNOW ANSYS POLYFLOW

### A.2.1 Structure

Ansys POLYFLOW is structured in different applications that interact through a platform called Workbench. First, the geometry is created in *DesignModeler*. Second, the mesh is updated through *Mesh*. Third, the problem is setup in *Polydata*. Fourth, the calculations are made with POLYFLOW code. Finally, results and post processing can be studied in *CFD-Post* (Ansys POLYFLOW 12.1 in workbench user's guide 2009; Ansys Meshing user's guide 2010; Ansys POLYFLOW 12.1 user's guide 2009).

The feedblock setup, from DesignModeler to post processing, is detailed in chapter 3. Simulations of the multiplier follow the same process.

It is important to note that the tracking of the interface between the fluids involve a moving interface boundary condition and therefore a remeshing technique. The 3D optimesh technique only on the 3-layered domain has been used. Details of this technique can be found in section 16.6 of POLYFLOW user's guide (Ansys POLYFLOW 12.1 user's guide 2009).

### A.2.2 EVSS interpolation technique

Viscoelastic models like the Phan-Tien Tanner (PTT) model introduce additional variables in to the usual pressure and velocity in Newtonian flows. An EVSS (Elastic Viscous Split Stress) interpolation has been chosen to solve the numerical problem. This corresponds to how the PTT model is built as explained in chapter 2. In fact, the total stress tensor **T** is split into a purely viscous component $\mathbf{T}_2$ and an elastic component $\mathbf{T}_1$. The EVSS method is cheap from the computational point of view (Van Shaftingen & Crochet, 1984; Rajagopalan *et al.* 1990; section 11.2.5 in Ansys POLYFLOW 12.1 user's guide 2009). This idea of using the EVSS interpolation method has also been used in de Paulo *et al.* (2007) in their attempt in finding a numerical technique to solve free-surface flows modeled by the PTT constitutive equations.

## A.3 ANSYS POLYFLOW TEST

To validate the software and ensure it was properly used, a series of simulations inspired by previous publications (Southern & Ballman 1973; Karagiannis *et al.* 1990; Torres *et al.* 1993; Gifford 1997) were run. Only the comparison to the results of Gifford (1997) featuring the coextrusion of two Newtonian fluids are presented here.

Figure A**.1** is a sketch of a channel and Figure A**.2** represents the idealized geometry in which two separate fluids are joined together. In the first part of the channel, the two fluids are fed in two different inputs with a plane separating them: fluid1 of viscosity $\mu_1$ at the bottom at a flow rate $Q_1$ and fluid 2 of viscosity $\mu_2$ on top at a flow rate $Q_2$

The separation plane is not through the whole domain. It is after their merging that an interface is formed and will be distorted downstream.

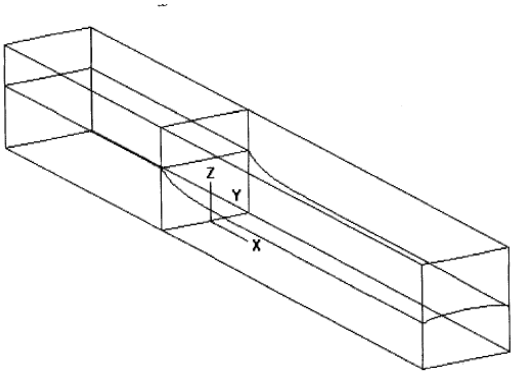


**Figure A.1.** Coextrusion in a square channel from Gifford (1997)

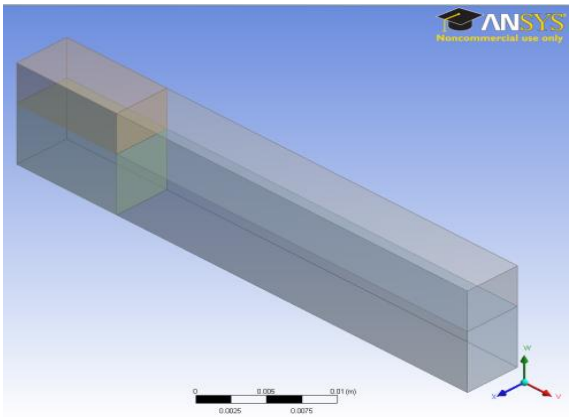


**Figure A.2**. DesignModeler equivalent geometry

Gifford produced different graphs showing his results. He showed the velocity profile of both his simulations results and the solution of the set of equation that defines the problem. We see his results and the simulated velocity profile match (Figure A.3; Figure A.4; Figure A.5).

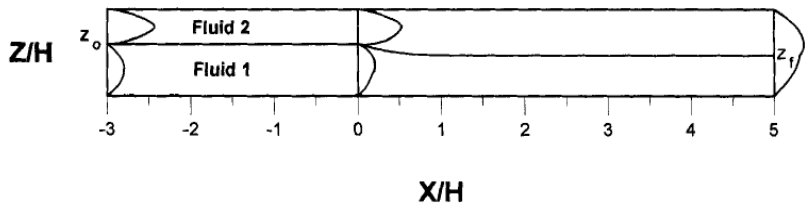


**Figure A.3.** 2D Coextrusion in a channel from Gifford (1997)

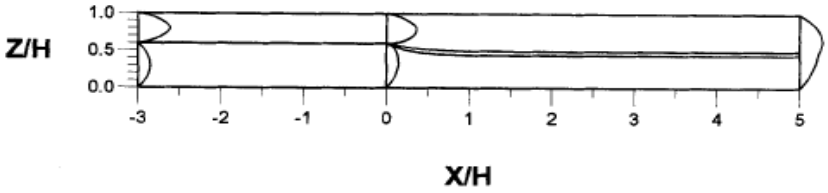


**Figure A.4**. Coextrusion in a square channel from Gifford (1997)

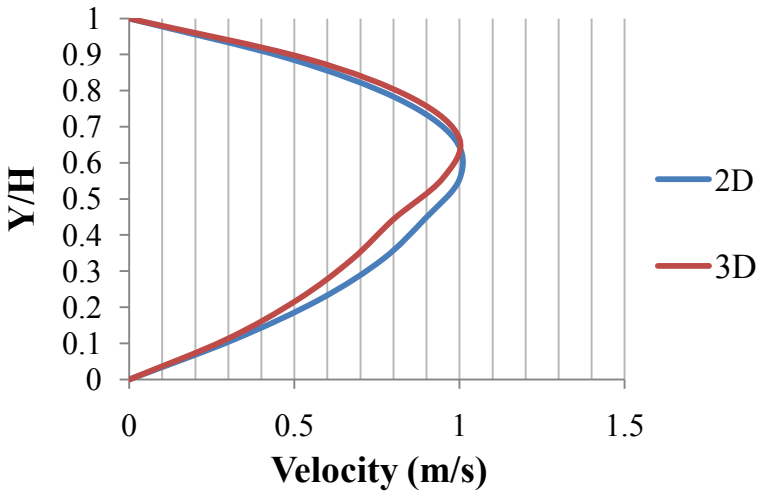


**Figure A.5.** Velocity profile for the simulation in 2D and 3D equivalent to Figure A.3 and Figure A.4 conducted by Gifford (1997)

Gifford also shows the final interface profile for the 2D problem (Figure A.6a and b) and for the 3D problem studying the effect of the flow rate ratio (Figure A.7a and b) and of the viscosity ratio (Figure A.8a and b) of the two fluids. Both results match very well quantitatively.

a.

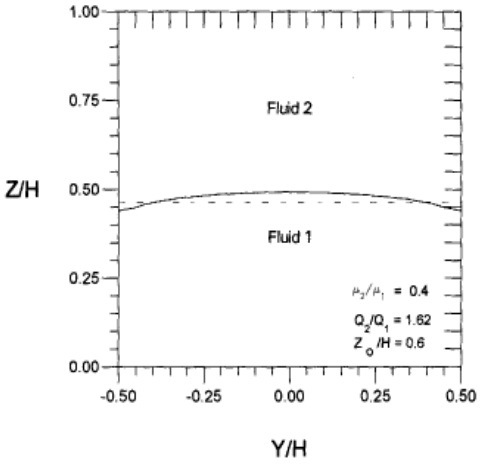


b.

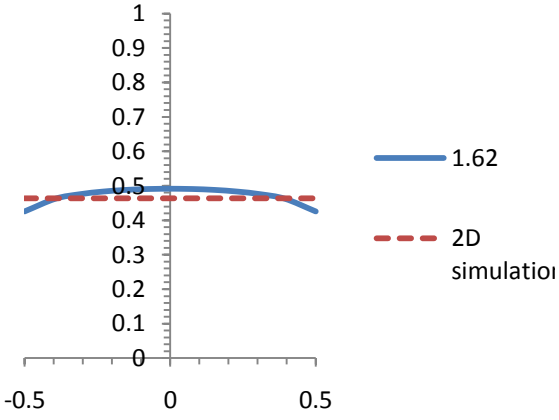


**Figure A.6.** a) Final interface profile in a square channel and a 2D channel ($\mu_2/\mu_1$=0.4; $Q_2/Q_1$=1.62) from Gifford (1997); b) Equivalent simulation to Figure A.6a in Ansys POLYFLOW.

a. b.

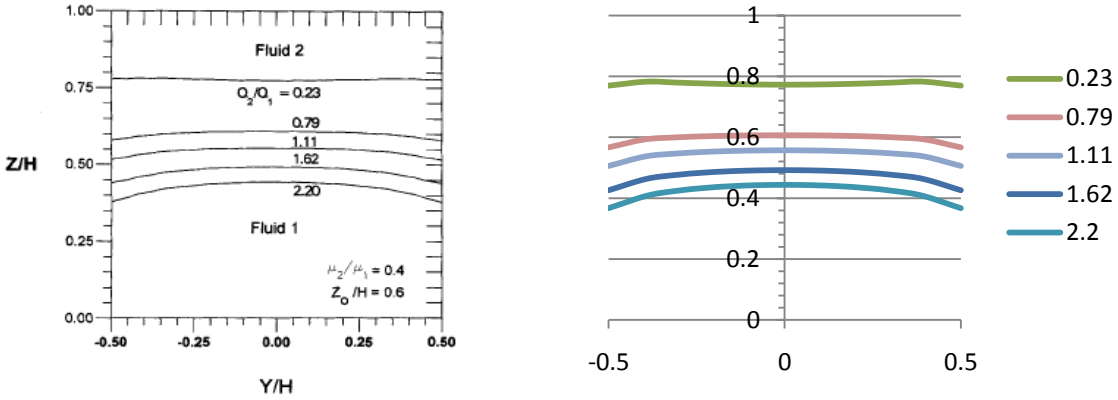


**Figure A.7**.a) Effect of the flow rate ratio $Q_2/Q_1$ on the interface profile ($\mu_2/\mu_1$=0.4) from Gifford (1997); b) Equivalent simulation to Figure A.7a in Ansys POLYFLOW.

a. b.

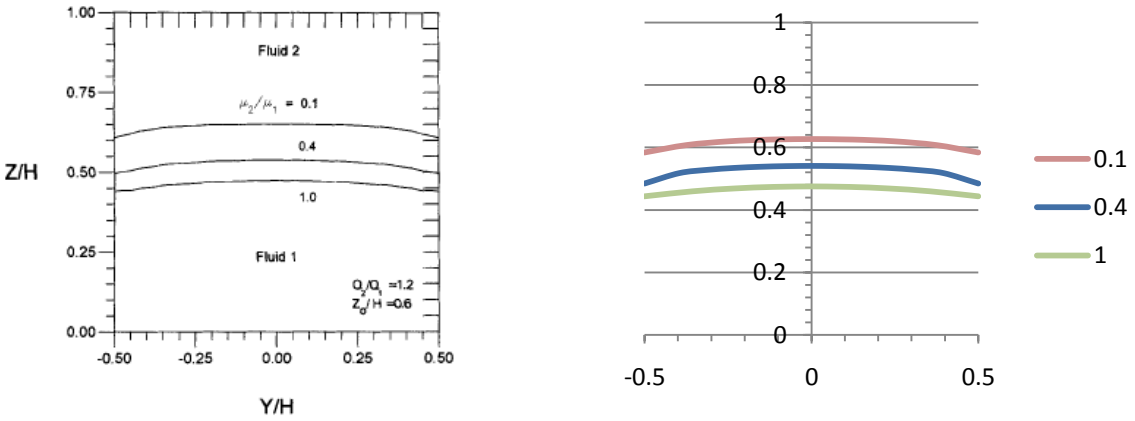


**Figure A.8**. a) Effect of the viscosity ratio $\mu_2/\mu_1$ on the interface profile ($Q_2/Q_1$=1.62) from Gifford (1997); b) Equivalent simulation to Figure A.8a in Ansys POLYFLOW.

## A.4 CONCLUSIONS

The agreement between the simulation and Gifford's results (Gifford 1997) provides some validation of Ansys Polyflow.

# References


Ansys Meshing user's guide, 2010

Ansys POLYFLOW 12.1 in workbench user's guide, 2009

Ansys POLYFLOW 12.1 user's guide, 2009

Ansys POLYFLOW 12.1 Examples Manual, 2009

Balta Calleja, Roslaniec, 2000, Block copolymers, CRC Press

Bluem G. L., Frankel J. M., Kramlich D. C., Brott R. L., Hart S. D., Lorimor L. E., Fleming P. R., Kopecky W. J., Wilson B. B., Jonza J. M., 2009, Color shifting multilayer polymer fibers and security articles containing color shifting multilayer polymer fibers, US. patent 20110096395

Carranza, 2010, Modeling of oxygen scavenging polymers and composites, PhD Dissertation

Chisholm D., Schrenk W. J., 1971, Method of Extruding Laminates, US. Patent 3,557,265

Cloeren technology, http://2.imimg.com/data2/RH/FC/MY-976935/coextrusion-technology.pdf

Debbaut B., Avalosse T., Dooley J., Hughes K., 1997, On the development of secondary motions in straight channels induced by the second normal stress difference: experiments and simulations, J. Non-Newtonian Fluid Mech., **69**, 2-3, 255-271

Dooley J, 2002, Viscoelastic Flow Effects in Multilayer Polymer Coextrusion, Eindhoven University of Technology

Everage A. E., 1975, Theory of Stratified Bicomponent Flow of Polymer Melts. II. Interface Motion in Transient Flow, Transactions of the society of rheology, **19**, 4, 509-522

Gifford W.A., 1997, A three-dimensional analysis of coextrusion, Poly. Eng. Sci., **37**, 2, 315-320

Gifford W.A., 2000, A Three-Dimensional Analysis of Coextrusion in a Single Manifold Flat Die, Poly. Eng. Sci., **40**, 9, 2095-2099

Karagiannis A., Hrymak A. N., Vlachopoulos J., 1990, Three-dimensional studies on bicomponent extrusion, Rheol. Acta, **29**, 1, 71-87

Khomami B., Wilson G. M., 1995, An experimental investigation of interfacial instability in superposed flow of viscoelastic fluids in a converging/diverging channel geometry, J. Non-Newtonian Fluid Mech., **58**, 47-65

Kynar Films, 2001, Novel PVDF Multilayer blown films

Li J., Suo J., Jia L., 2010, Morphologies and mechanical properties of Organic-Inorganic Multilayered Composites, Pol. Eng. Sc., **50**, 4, 689-696

McCrum, Buckley, Bucknall, 1997, Principles of Polymer Engineering, chapter 6, 2nd ed., Oxford Science publication

Paulo (de) G. S., Tome M. F., Mc Kee S., 2007, A Marker-and-cell Approach to Viscoelastic Free Surface Flows Using the PTT model, Journal of non-Newtonian Fluid Mechanics, **147**, 3, 149-174

Pethe V., Wang H. P., Hiltner A., Baer E., Freeman B. D., 2008**,** Oxygen and Carbon Dioxide Permeability of EAA/PEO Blends and Microlayers J. App. Pol. Sc., **110**, 1411-1419

Phan Thien N., Tanner R. I., 1977, A new constitutive equation derived from network theory, J. Non-Newt. Fluid Mech, **2**, 4, 353-365

Ponting M., Hiltner A., Baer E., 2010a, Polymer nanostructures by forced assembly: process, structure, and properties, Macromol. Symp., **294-1**,19-32

Ponting M., Burt T., Korley L. T. J., Andrews J., Hiltner A., Baer E., 2010b, Gradient Multilayer Films by Forced Assembly Coextrusion, Ind. Eng. Chem. Res., **49**, 12111-12118

Rajagopalan D., Armstrong R. C., Brown R. A., 1990, Finite-element methods for calculation of steady, viscoelastic flow using constitutive equations with a Newtonian viscosity , J. Non-Newtonian Fluid Mechanics, **36**, 159-192

Raley G.E., 1965, Melt Extrusion of Multi-Wall Plastic Tubing, U.S. Patent 3,223,761

Ramanathan, R., Shanker, R., Rehg, T., Jons, S., Headley, D.L. and Schrenk, W.J., 1996, Wave Pattern Instability in Multilayer Coextrusion – An Experimental Investigation, SPE-ANTEC Technical Papers, **42**, 224

Robeson L. M., 2007, Polymer blends: a comprehensive review, Hanser Verlag

Samuel I.D.W., 2004, Laser Physics: Fantastic plastic, Nature, **429**, 709-711

Schrenk W.J, Shastri R. K., Ayres R.E., 1992, Methods and apparatus for generating interfacial surfaces, US. Patent 5,094,793

Singer K. D., Kazmierczak T., Lott J., Song H., Wu Y., Andrews J., Baer E., Hiltner A., Weder C., 2008, Melt-process, All-polymer, Distributed Bragg Reflector Laser, Optics Express, **16**, 14, 10358-10363

Song H., Singer K., Lott J., Wu Y., Zhou J., Andrews J., Caer E., Hiltner A., Weder C., 2009, J. Mater. Chem., **19**, 7520-7524

Southern J. H., Ballman L. R., 1973, Stratified bicomponent flow of polymer melts in a tube, Appl. Pol. Sci. B, **20,** 175-189

Strobl Gert R., 2007, The Physics of Polymers: Concepts for Understanding Their Structures and Behavior, Section 3.2 Polymer Mixtures, 3rd edition, Springer

Su Y. Y., B. Khomami, 1992a, Interfacial Stability of Multilayer Viscoelastic Fluids in Slit and Converging Channel Die Geometries, J. Rheol., **36**, 357-387

Su Y. Y., B. Khomami, 1992b, Purely Elastic Interfacial Instabilities in Superposed Flow of Polymeric, Fluids Rheol. Acta, **31**, 413

Tanoue S, Naganawa T., Iemoto Y., 2006, Quasi-three dimensional Simulation of Viscoelastic Flow through a Straight Channel with a Square Cross Section, Nihon Reoroji Gakkaishi, **34**, 2, 105-113

Torres A., Hrymak A. N., Vlachopoulos J., Dooley J., Hilton B. T., 1993, Boundary conditions for contact lines in coextrusion flows, Rheol. Acta, **32**, 513-525

Utracki, 2002, Polymer Blends Handbook Vol. 1, Kluwer Academic Publsihers, Springer

Van Shaftingen J. J., Crochet M. J., 1984, A comparison of mixed Methods for solving the flow of a Maxwell fluid, International journal for numerical methods in fluids, **4**, 11, 1065-1081

Wang H., Keum J. K., Hiltner A., Baer E., 2009, Confined Crystallization of PEO in Nanolayered Films Impacting Structure and Oxygen Permeability, Macromolecules, **42**, 7055-7066

White J. L., Lee B., 1975, Theory of interface distortion in stratified two-phase flow, Trans. Soc. Rheol. **19**, 457

Wilson G. M., Khomami B., 1993, An experimental investigation of interfacial instabilities in multilayer flow of viscoelastic fluids. II. Elastic and nonlinear effects in incompatible polymer systems, J. Rheol, **37**, 2, 315-339

Wooddell G. L., 1980, Characteristics of Multilayer Structures Prepared by Coextrusion extrusion coating , TAPPI Paper Synthetics Proceedings, 119

Xie Z., Huang J., Li C., Xiao B., Liu S., Li d., 1999, Multilayer organic leds based on a new dye-doped polymer, Chinese J. Pol. Sci., **17**, 4, 343-346

Yue P., Zhou C., Dooley J., Feng J.J., 2008, Elastic encapsulation in bicomponent stratified flow of viscoelastic fluids, J. Rheol., **52**, 4, 1027-1042

# Vita

Erwan Chabert was born and raised in France. He attended Graduate School at The University of Texas at Austin in a double degree program with the Ecole Centrale de Lille where he studied two years after his studies in preparatory classes at Lycee Marcelin Berthelot.

Permanent email: erwan.chabert@utexas.edu

This thesis was typed by the author.